Electronic Supplementary Information

Ultrafast Channel II Process Induced by a 3-D Texture with Enhanced Acceptor Order Ranges for High-Performance Non-Fullerene Polymer Solar Cells

Shanshan Chen,[†,a] Sang Myeon Lee,[†,a] Jianqu Xu[†,b], Jungho Lee,[†,a] Kyu Cheol Lee,[a,c] Tianyu Hou,[d] Yankang Yang,[e] Mingyu Jeong,[a] Byongkyu Lee,[a] Yongjoon Cho,[a] Sungwoo Jung,[a] Jiyeon Oh,[a] Zhi-Guo Zhang,[e] Chunfeng Zhang,[b] Min Xiao,[b] Yongfang Li,[e] Changduk Yang*[,a]

[a.] Department of Energy Engineering, School of Energy and Chemical Engineering, Perovtronics Research Center, Low Dimensional Carbon Materials Center, Ulsan National Institute of Science and Technology (UNIST), 50 UNIST-gil, Ulju-gun, Ulsan 44919, South Korea.

[b.] National Laboratory of Solid State Microstructures, School of Physics, and Collaborative Innovation Center of Advanced Microstructures, Nanjing University, Nanjing 210093, China

[c.] Research Center for Green Fine Chemicals, Korea Research Institute of Chemical Technology, Ulsan 44412, Republic of Korea.

[d.] Key Laboratory of Flexible Electronics (KLOFE) & Institute of Advanced Materials (IAM), Jiangsu National Synergetic Innovation Center for Advanced Materials (SICAM), Nanjing Tech University (NanjingTech), Nanjing 211816, China.

[e.] Beijing National Laboratory for Molecular Sciences, CAS Key Laboratory of Organic Solids, Institute of Chemistry, Chinese Academy of Sciences, Beijing 100190, China.

*. yang@unist.ac.kr

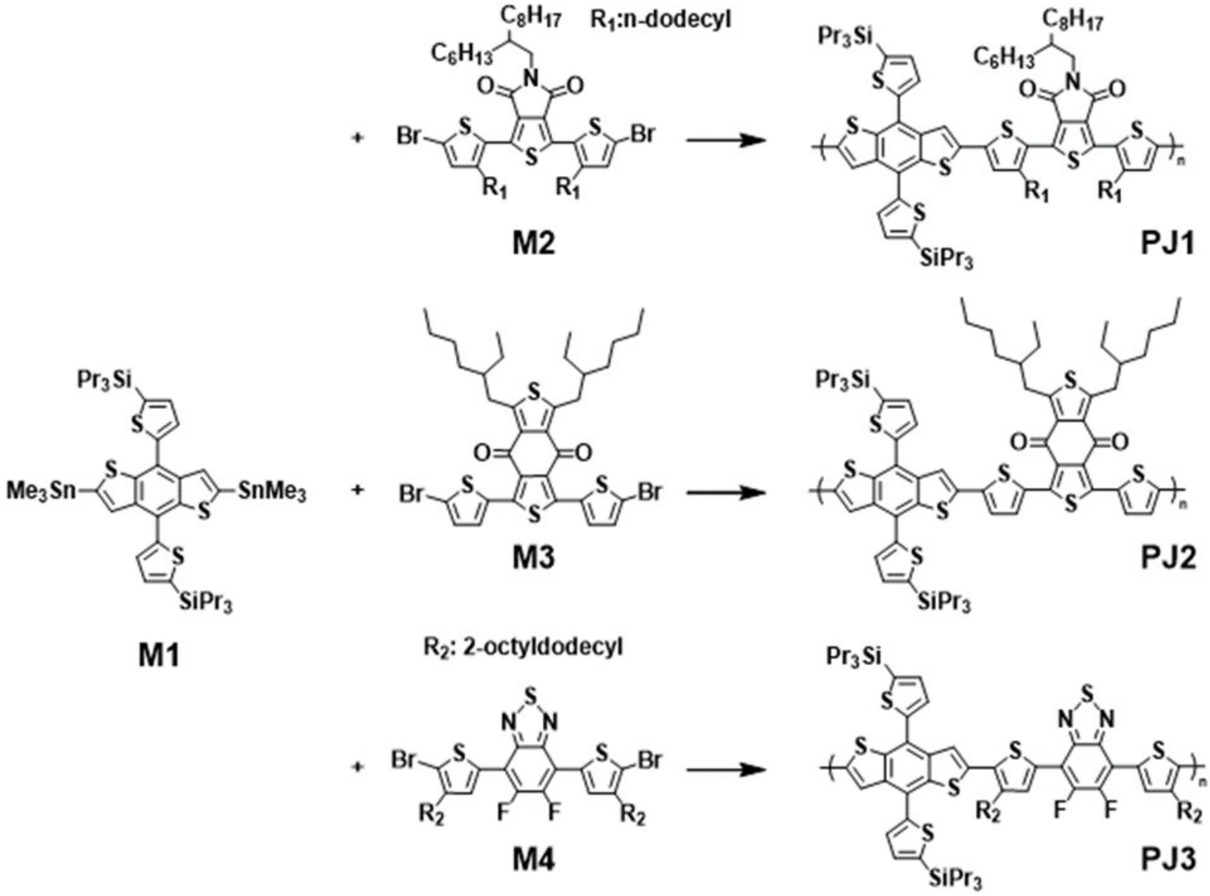

Scheme S1 Synthetic routes for polymer donors PJ1, PJ2, and PJ3.

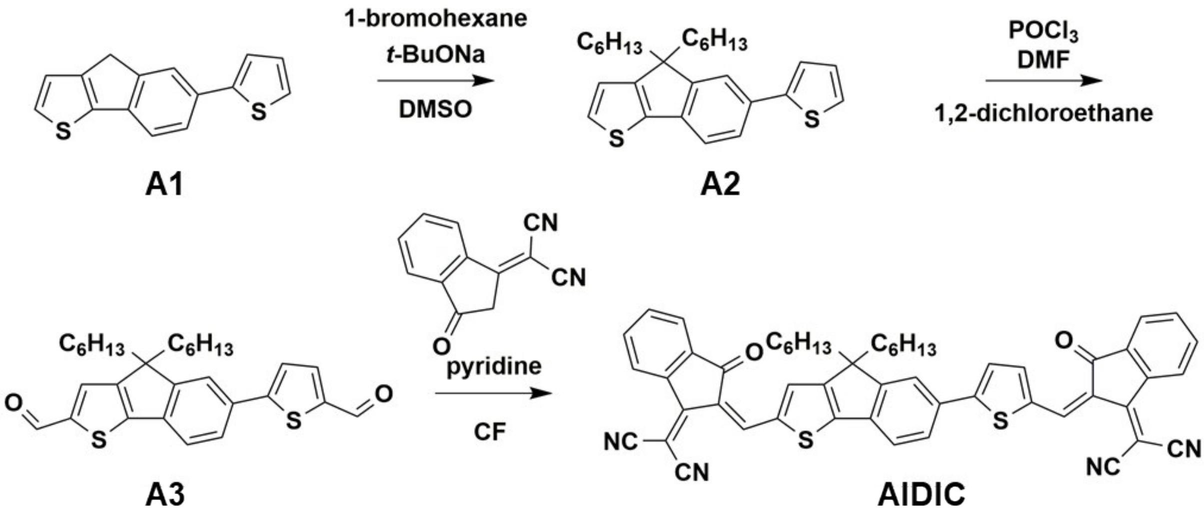

Scheme S2 Synthetic routes for small molecular acceptor AIDIC.

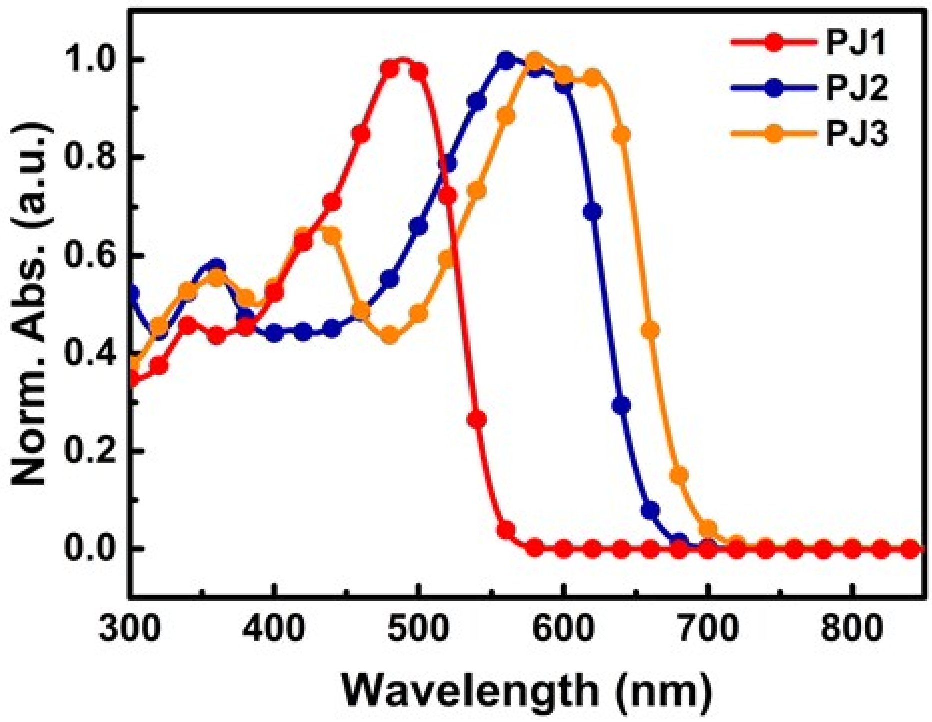

Fig. S1 UV-Vis absorption spectra of the polymer donors in chloroform.

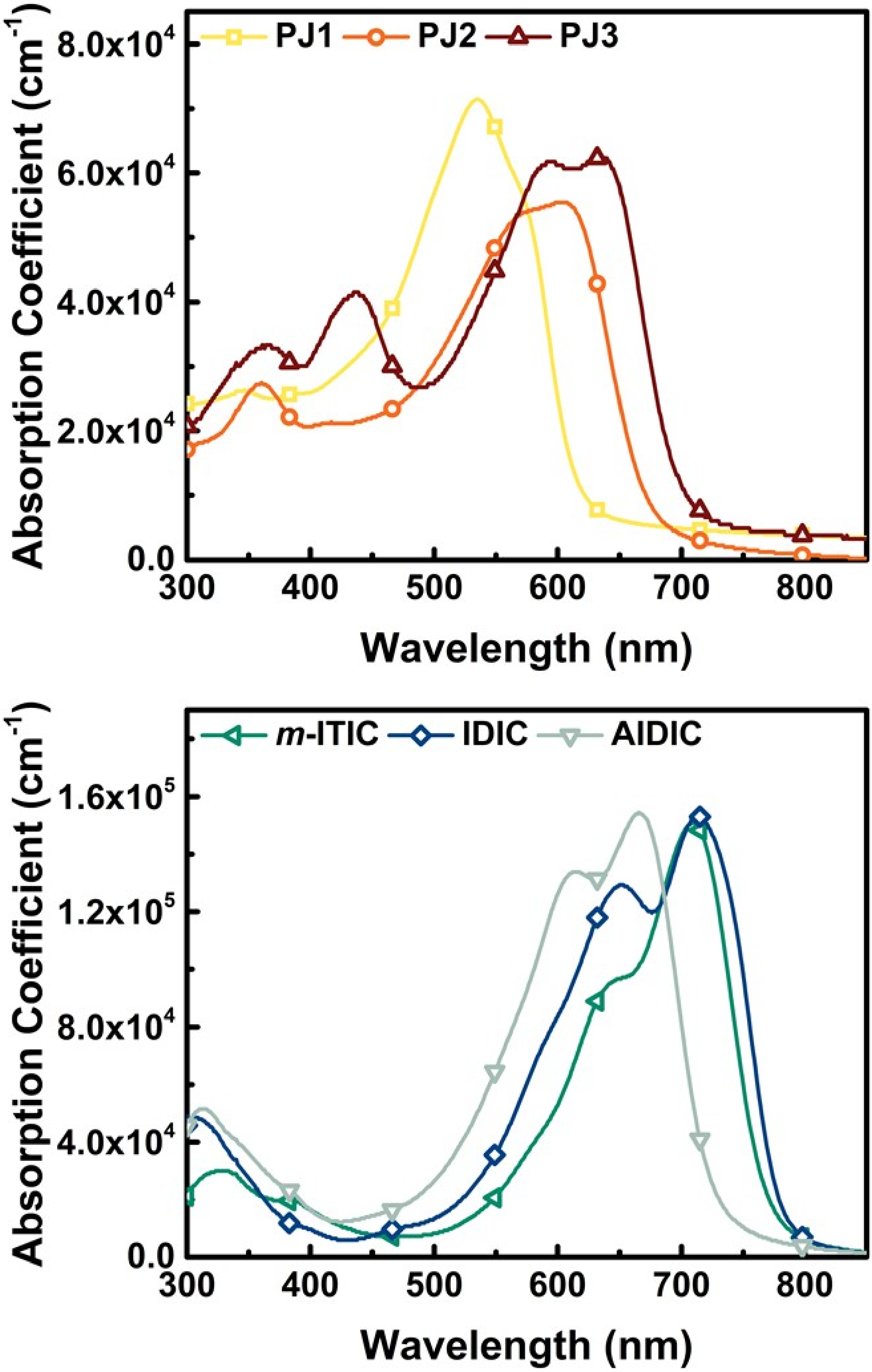

Fig. S2 UV-Vis absorption spectra of neat films.

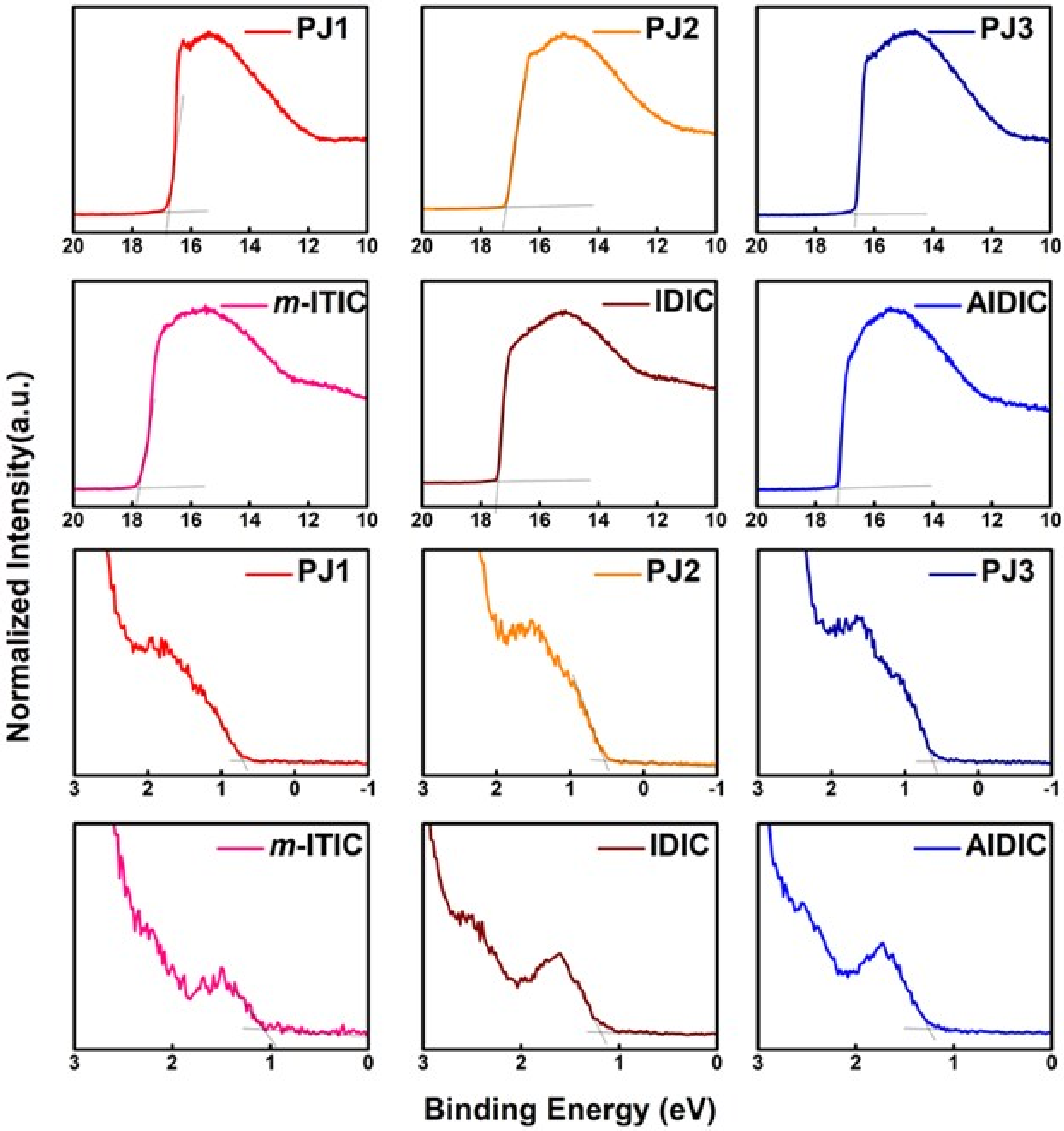

Fig. S3 The UPS spectra of the polymer donors and small molecular acceptors films.

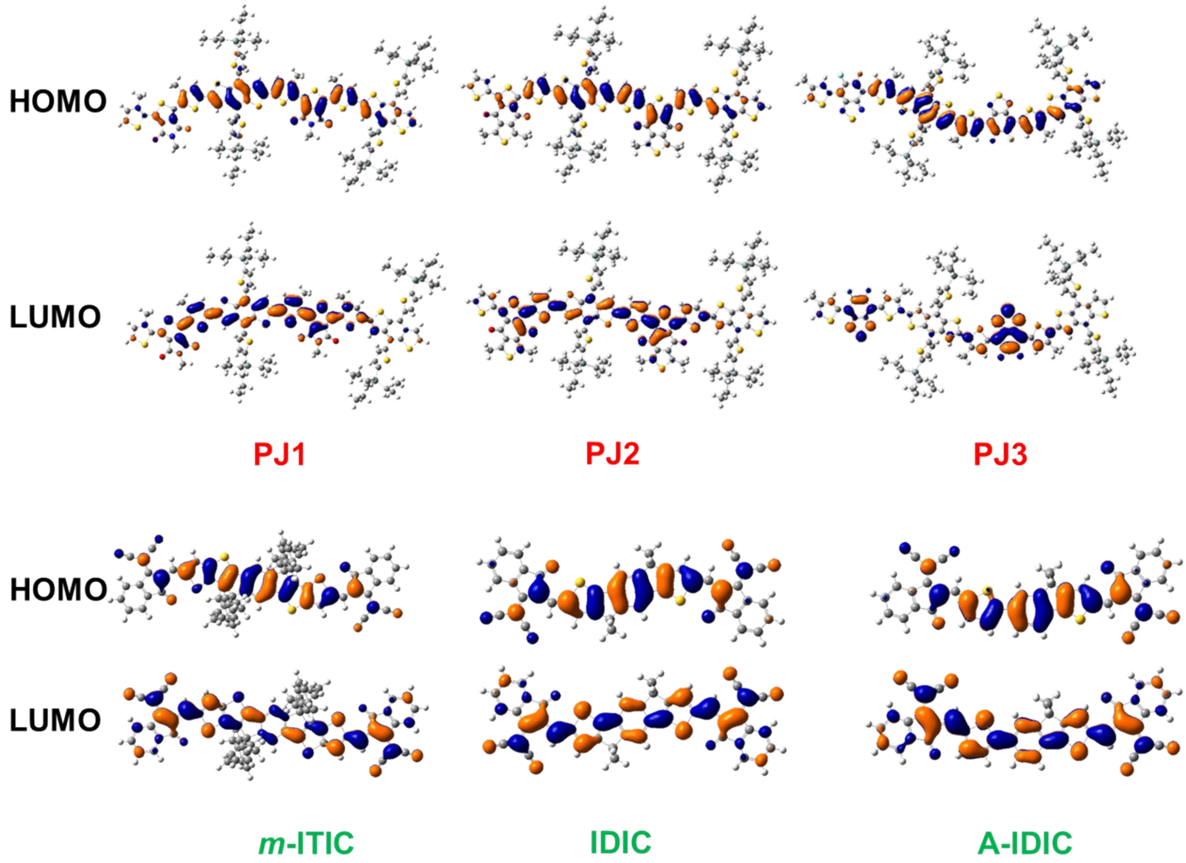

Fig. S4 The optimized frontier orbitals of the polymer donors and small molecular acceptors at the level of B3LYP/6-31 G* basis set.

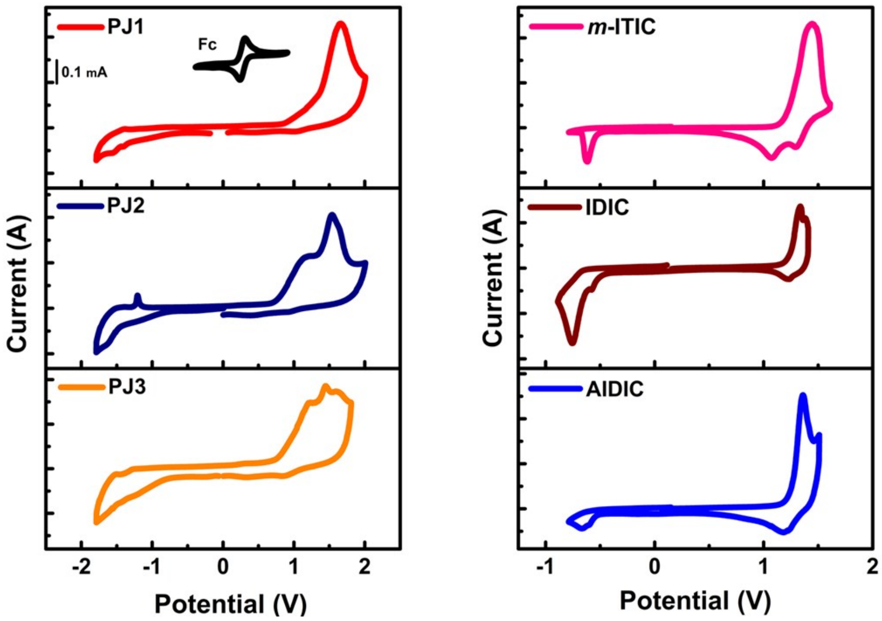

Fig. S5 The cyclic voltammetry (CV) curves of the polymer donors and small molecular acceptors films at a scan rate of 50 mV s^{-1}.

Table S1 The density functional theory (DFT) calculations- and cyclic voltammetry (CV)-derived energy levels of polymer donors and small molecular acceptors.

Sample	DFT		CV	
	E_{HOMO} (eV)	E_{LUMO} (eV)	E_{HOMO} (eV)	E_{LUMO} (eV)
PJ1	-5.12	-2.83	-5.55	-3.60
PJ2	-4.89	-2.73	-5.45	-3.58
PJ3	-4.53	-2.70	-5.42	-3.57
m-ITIC	-5.53	-3.44	-5.68	-3.95
IDIC	-5.64	-3.60	-5.71	-4.00
AIDIC	-5.70	-3.52	-5.75	-3.96

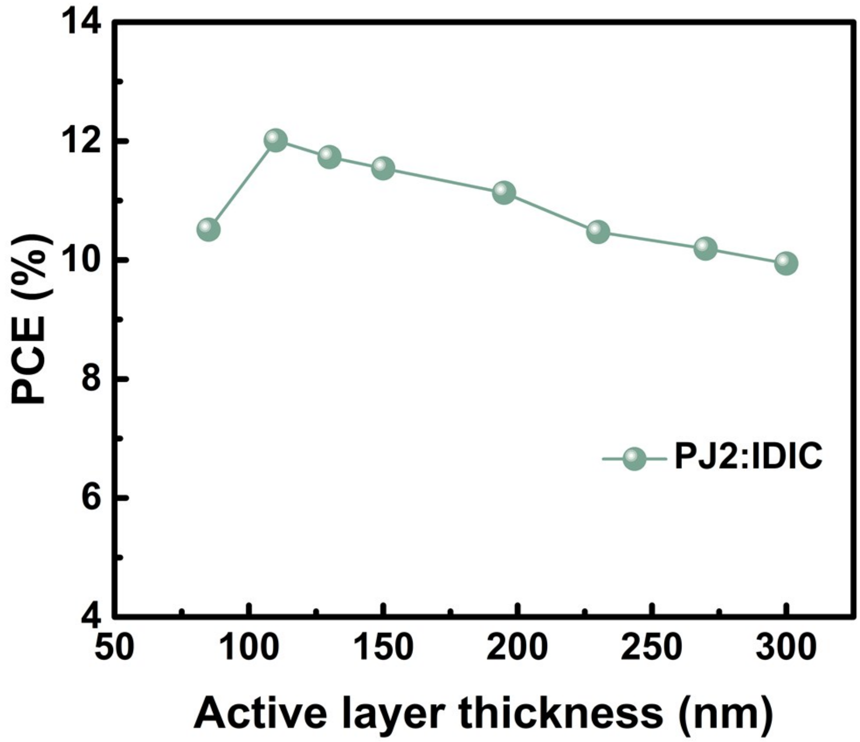

Fig. S6 Thickness dependence of the PJ2:IDIC photovoltaic performance.

Table S2 Effect of the active layer thickness on the photovoltaic performance of the PSCs based on PJ2: IDIC.

Thickness [nm]	V_{OC} [V]	J_{SC} [mA cm-2]	FF [%]	PCE [%]
85	0.934	14.9	75.4	10.51
110	0.939	17.0	75.3	12.01
130	0.937	16.8	74.3	11.73
150	0.937	16.8	73.5	11.54
195	0.934	16.5	72.2	11.13
230	0.926	16.3	69.5	10.47
270	0.923	17.8	62.1	10.19
300	0.922	18.0	60.0	9.94

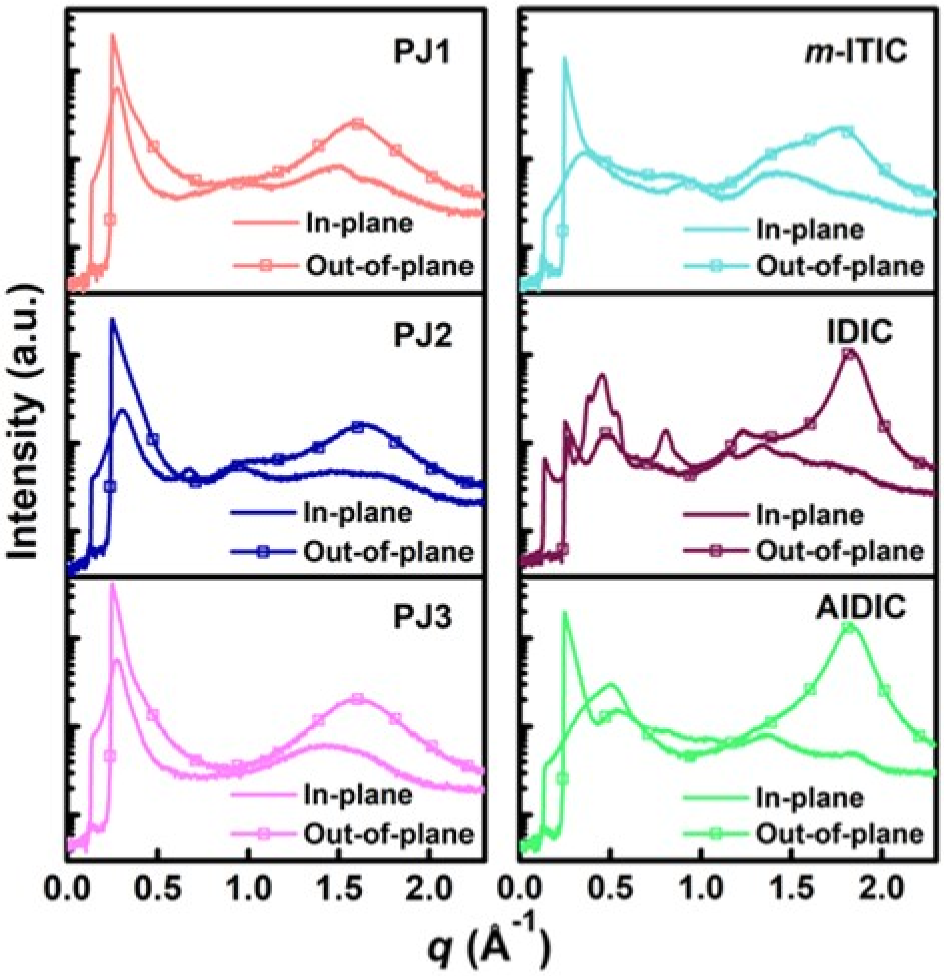

Fig. S7 Line cuts of the GIWAXS images of the neat polymer donors and small molecular acceptors films.

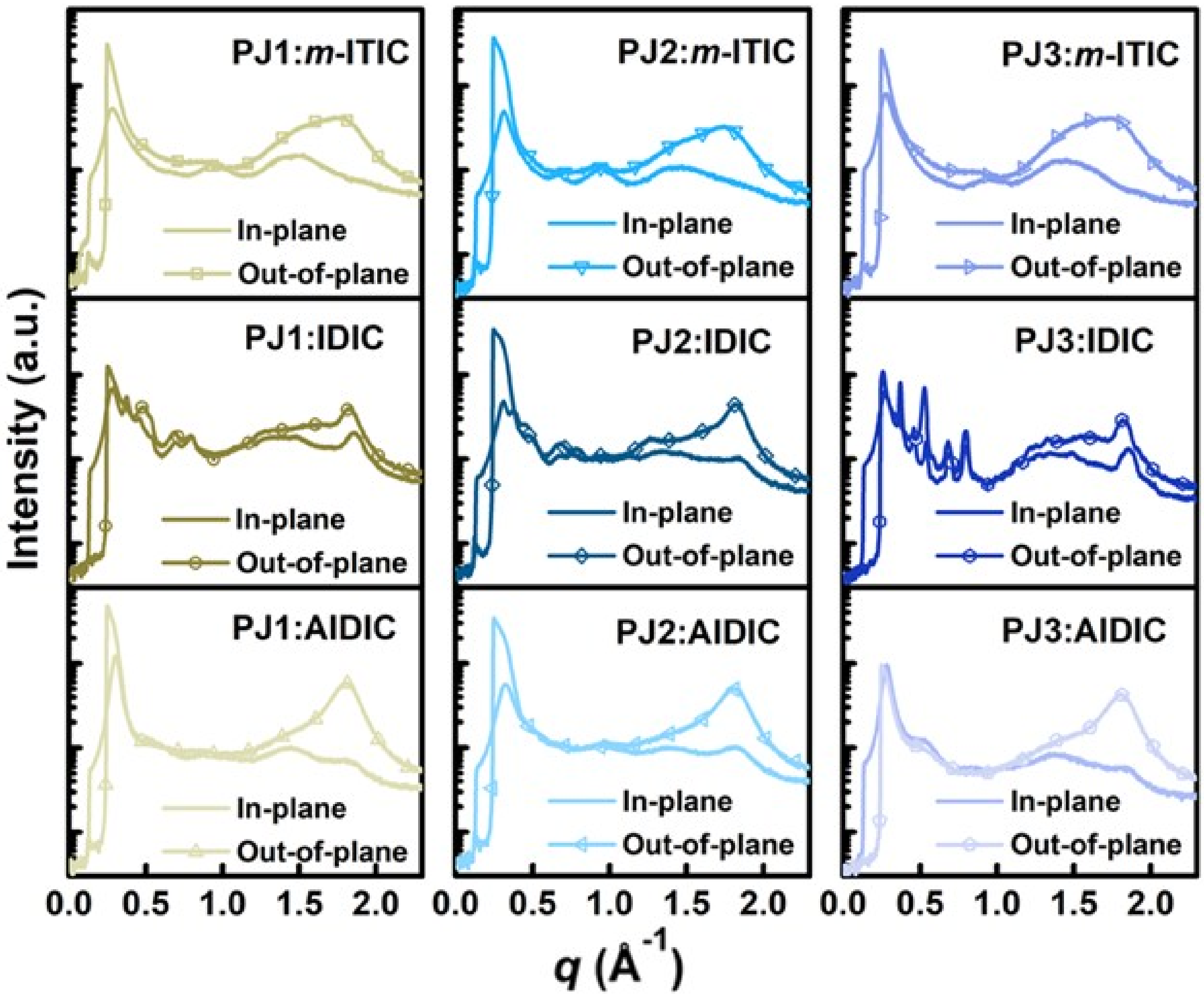

Fig. S8 Line cuts of the GIWAXS images of the blend films.

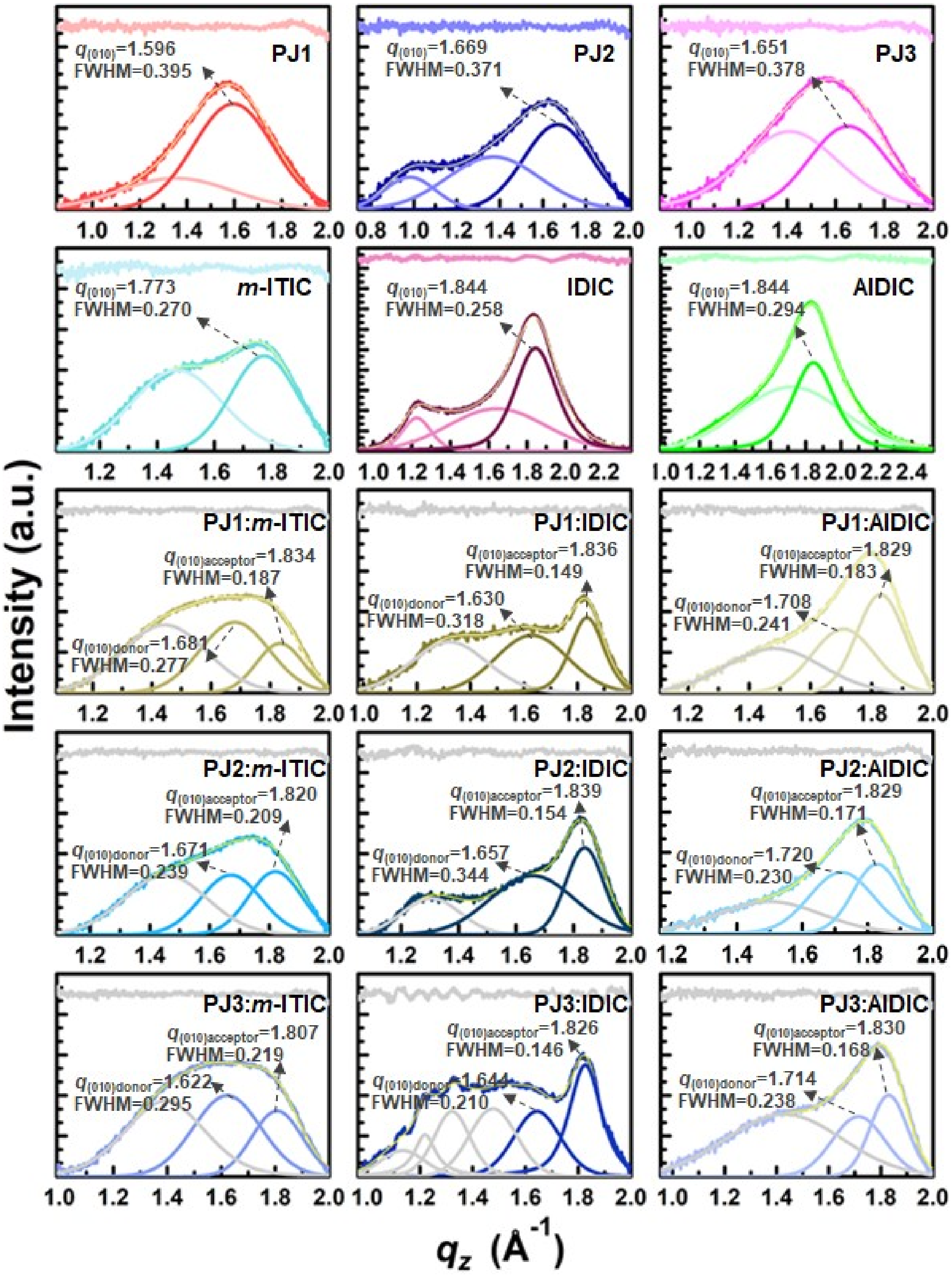

Fig. S9 Multi-peak fits of the out-of-plane GIWAXS line cuts at the high region for the neat and blend films.

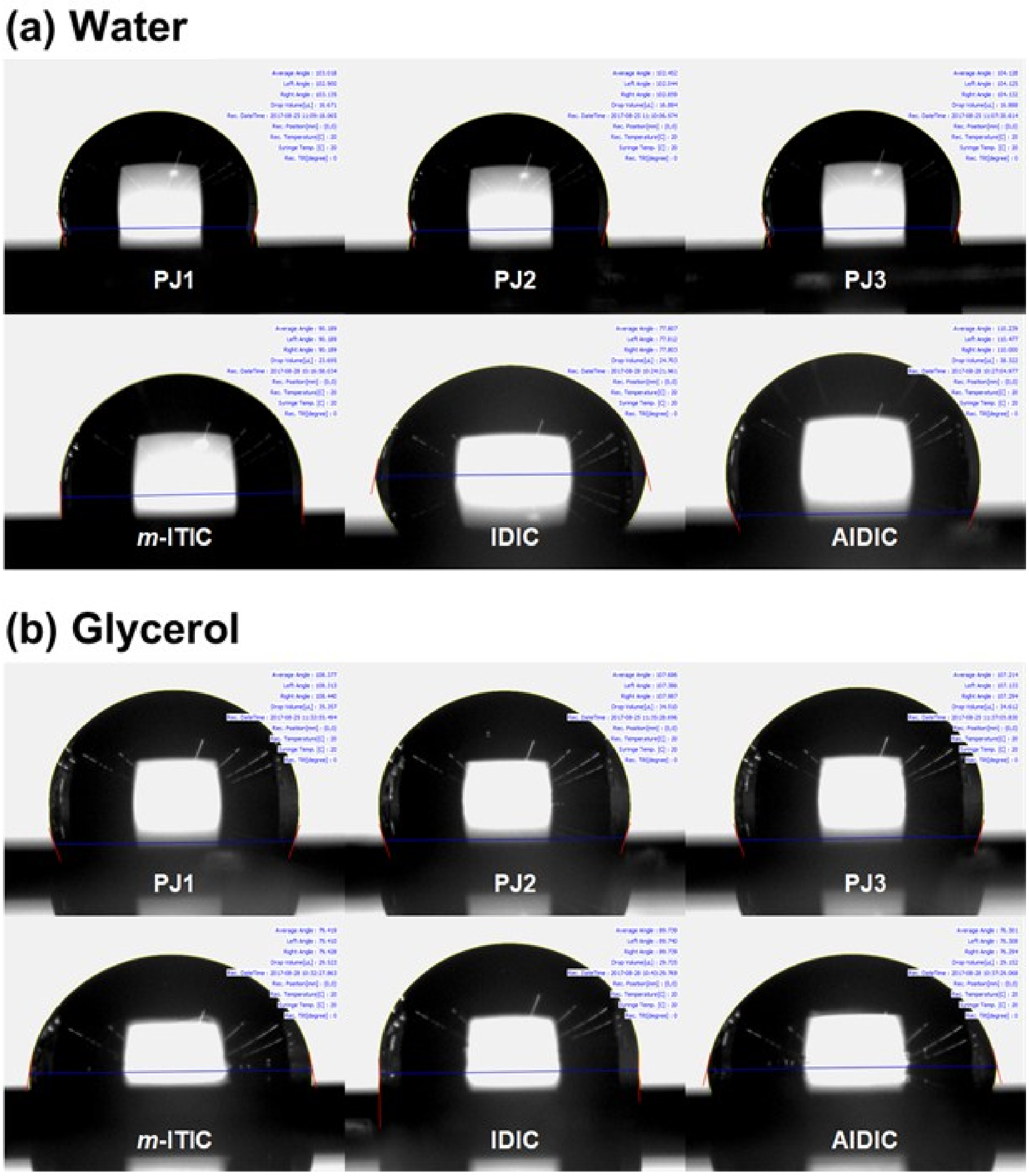

Fig. S10 Contact angle measurement images of the neat donor polymers and small molecular acceptors films by using water and glycerol.

Table S3 Contact angles and calculated surface tensions of neat donor polymers and SMAs and the interfacial tensions in pairs.

Sample	ϑ_{water} [deg]	$\vartheta_{glycerol}$ [deg]	Surface tension [mN m^{-1}]	Interfacial tension [mN m^{-1}]		
PJ1	103.018	108.377	20.498	22.227[a]	0.792[b]	126.333[c]
PJ2	102.452	107.686	20.622	21.510[a]	0.246[b]	125.685[c]
PJ3	104.128	107.214	18.464	23.082[a]	6.879[b]	120.043[c]
m-ITIC	90.189	79.419	26.645	—	—	—
IDIC	77.807	89.739	37.974	—	—	—
AIDIC	110.239	76.301	77.132	—	—	—

[(a)]The interfacial tension values of donor polymer:*m*-ITIC; [(b)]The interfacial tension values of donor polymer:IDIC; [(c)]The interfacial tension values of donor polymer:AIDIC.

Calculation of Surface Tensions between donor polymer and SMA

The surface tensions between donor polymer and SMA were calculated via measuring the contact angles of two different solvents (glycerol and water) on the each neat film. The surface tension of film was calculated via the Wu model and the following equations.[1]

$$\gamma_{water}(1+cos\theta_{water}) = \frac{4\gamma^{d}_{water}r^{d}}{\gamma^{d}_{water}+r^{d}} + \frac{4\gamma^{P}_{water}r^{P}}{\gamma^{P}_{water}+r^{P}}$$

$$\gamma_{glycerol}(1+cos\theta_{glycerol}) = \frac{4\gamma^{d}_{glycerol}r^{d}}{\gamma^{d}_{glycerol}+r^{d}} + \frac{4\gamma^{P}_{glycerol}r^{P}}{\gamma^{P}_{glycerol}+r^{P}}$$

$$\gamma^{total} = \gamma^{d} + \gamma^{P}$$

where $\gamma^{total}$is the total surface tension of material; $\gamma^{d}$and $\gamma^{P}$are the dispersion and polar components of γ^{total}, respectively; $\gamma_i$is the total surface tension of material *i*, where *i* = glycerol or water; $\gamma^{d}_{i}$and γ^{p}_{i}a are the dispersion and polar components of γ_i, respectively; ϑ is the contact angle measured.

The interfacial tension between the donor polymer and SMA was calculated using the following equation.[2]

$$\gamma_{12} = \gamma_1 + \gamma_2 - \frac{4\gamma^{d}_{1}4\gamma^{d}_{2}}{\gamma^{d}_{1}+\gamma^{d}_{2}} - \frac{4\gamma^{p}_{1}4\gamma^{p}_{2}}{\gamma^{p}_{1}+\gamma^{p}_{2}}$$

Where γ_{12} is the interfacial tension between two materials ; γ_j is the surface tension of material *j*, where *j* = 1 or 2, and as γ^{d}_{j} and γ^{p}_{j} are the dispersion and polar components of γ_j.

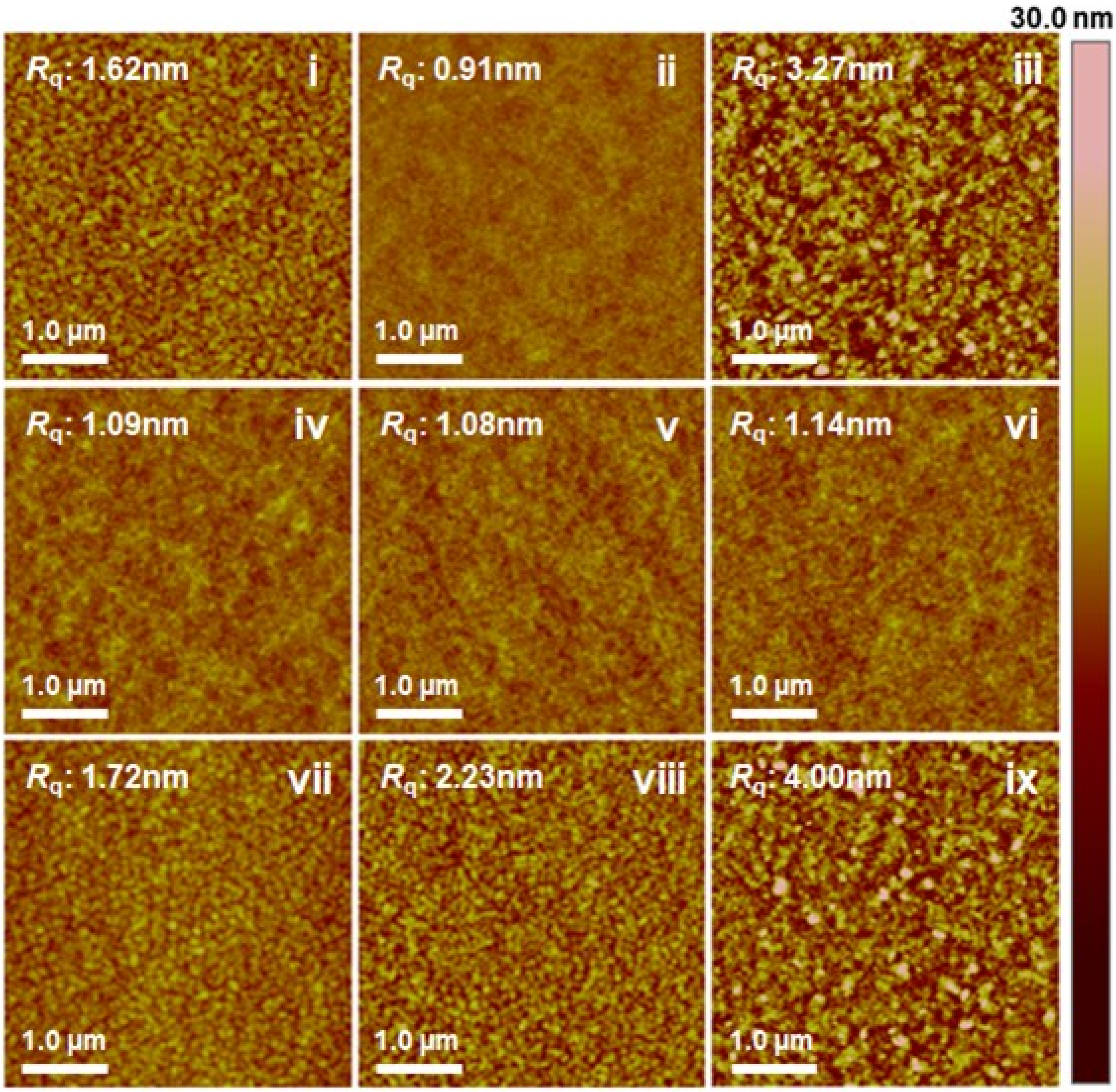

Fig. S11 AFM height images of the blend films: (i) PJ1:*m*-ITIC, (ii) PJ1:IDIC, (iii) PJ1:AIDIC, (iv) PJ2:*m*-ITIC, (v) PJ2:IDIC, (vi) PJ2:AIDIC, (vii) PJ3:*m*-ITIC, (viii) PJ3:IDIC, (ix) PJ3:AIDIC.

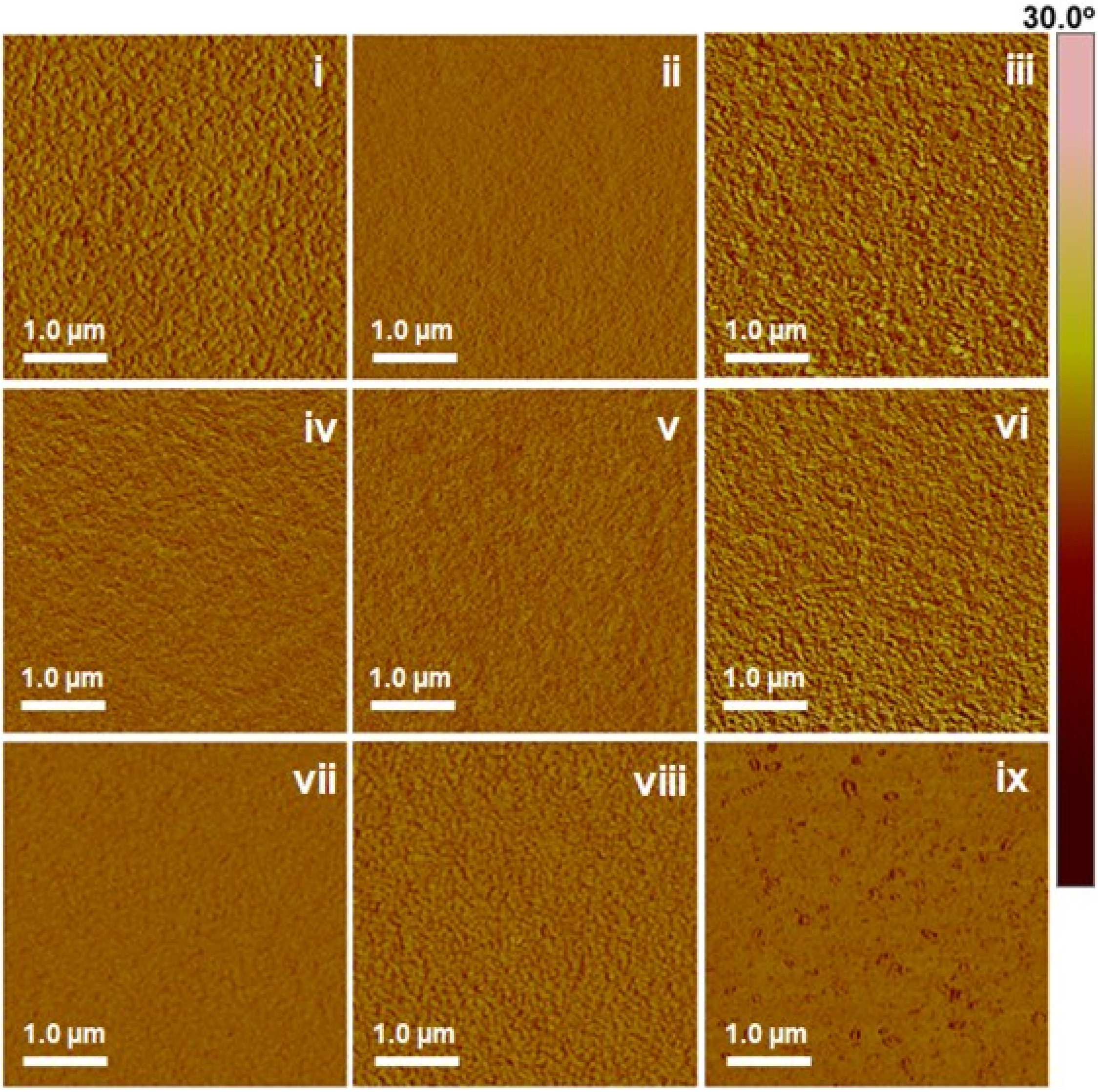

Fig. S12 AFM phase images of the blend films: (i) PJ1:*m*-ITIC, (ii) PJ1:IDIC, (iii) PJ1:AIDIC, (iv) PJ2:*m*-ITIC, (v) PJ2:IDIC, (vi) PJ2:AIDIC, (vii) PJ3:*m*-ITIC, (viii) PJ3:IDIC, (ix) PJ3:AIDIC.

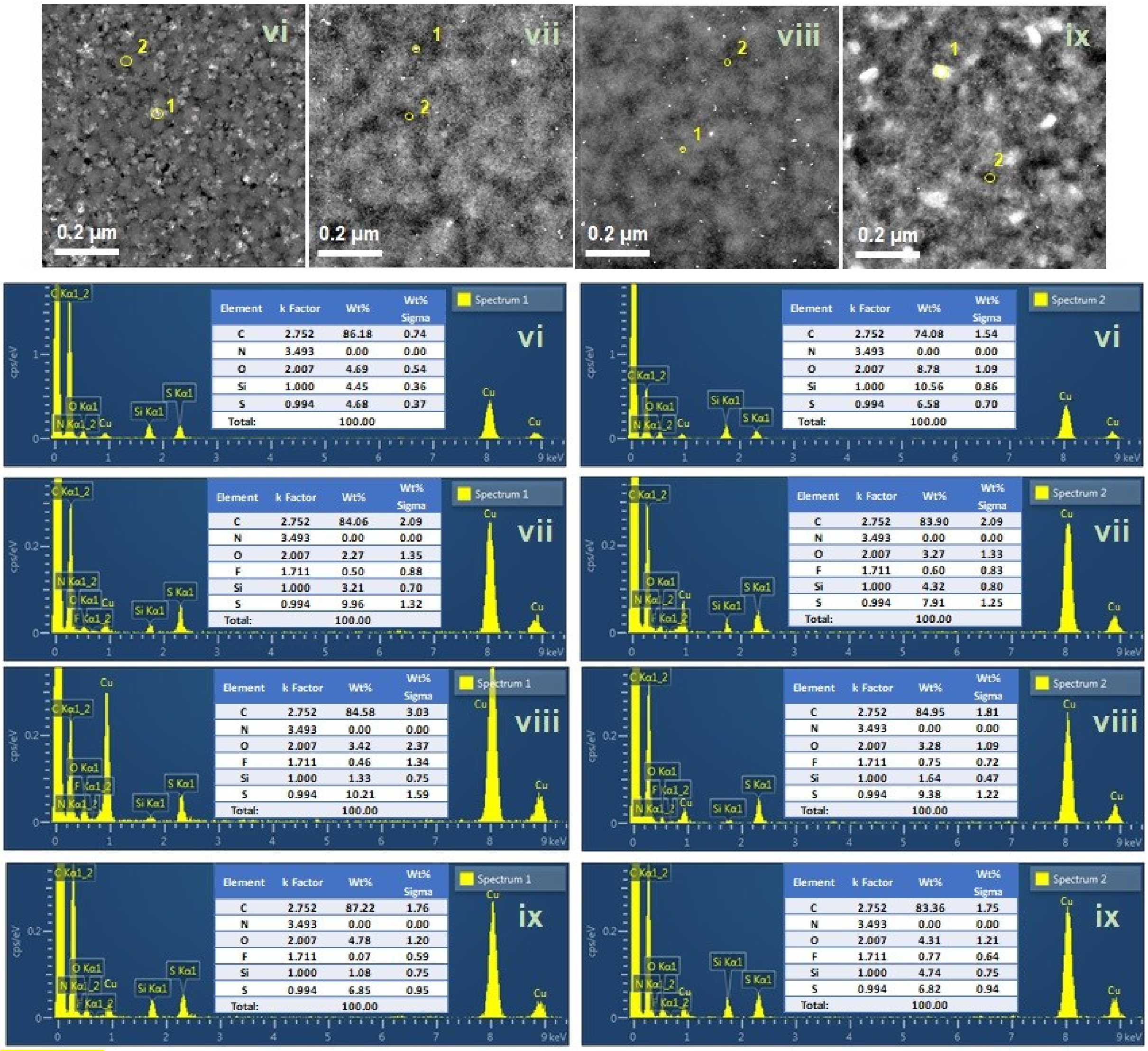

Fig. S13 The representative EDS spectrums and corresponding elemental ratio output for the bright (spectrum 1) and dark (spectrum 2) regions in blend films: (vi) PJ2:AIDIC, (vii) PJ3:*m*-ITIC, (viii) PJ3:IDIC, and (ix) PJ3:AIDIC.

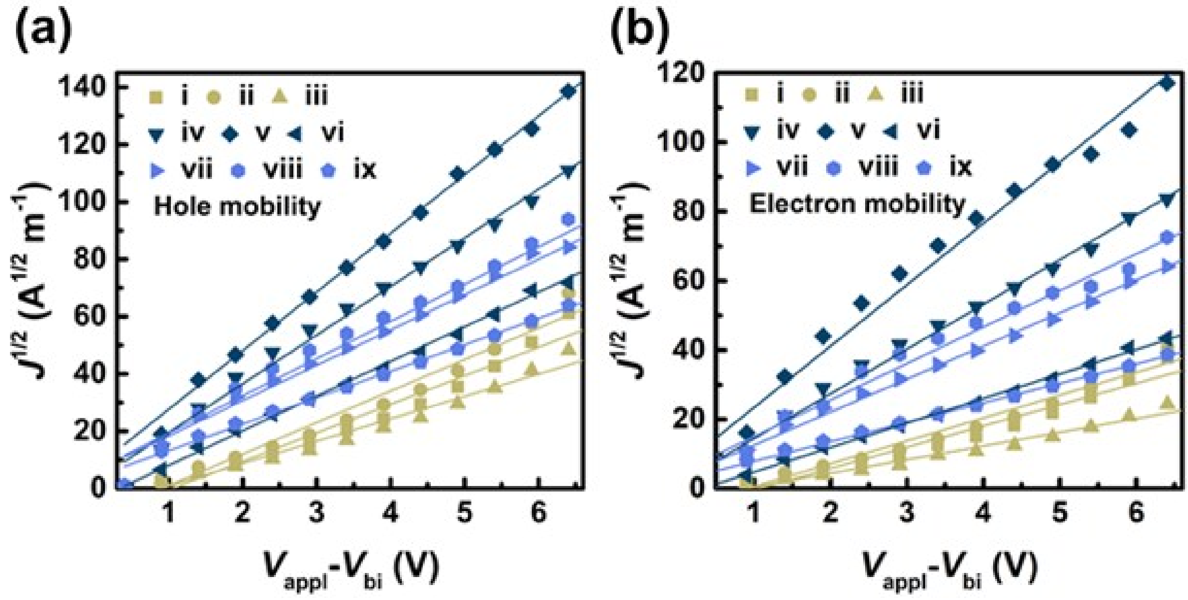

Fig. S14 $J^{1/2}$-V characteristic for the (a) hole-only and (b) electron-only devices based on the optimized blend films: (i) PJ1:*m*-ITIC, (ii) PJ1:IDIC, (iii) PJ1:AIDIC, (iv) PJ2:*m*-ITIC, (v) PJ2:IDIC, (vi) PJ2:AIDIC, (vii) PJ3:*m*-ITIC, (viii) PJ3:IDIC, (ix) PJ3:AIDIC.

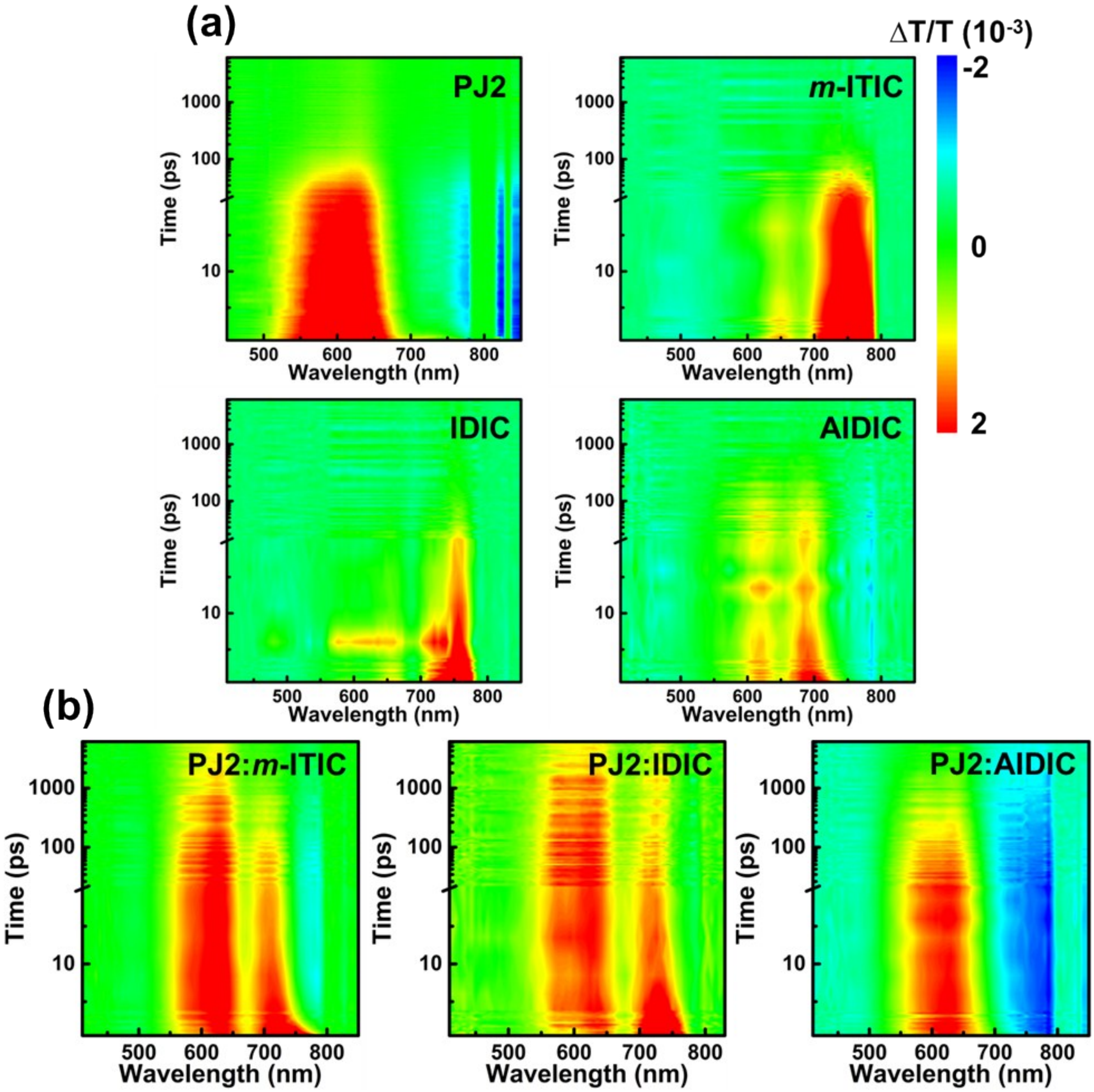

Fig. S15 (a) TA dynamics recorded from neat PJ2 with pump at 500 nm and neat small molecular acceptors with pump at 740 nm, and (b) corresponding blend films with pump at 740 nm.

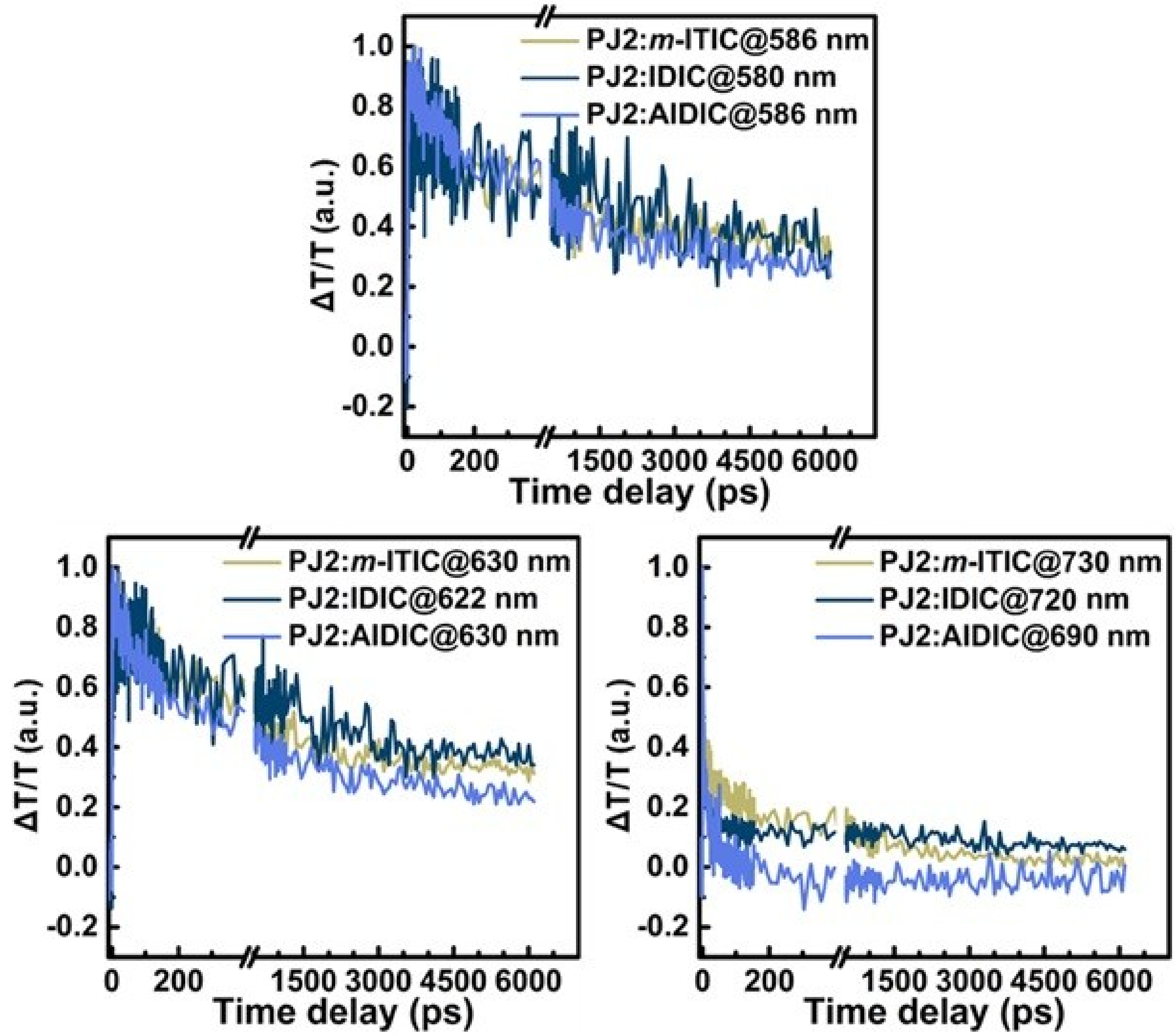

Fig. S16 TA dynamic curves probed at corresponding GSB signals arising from hole transfer.

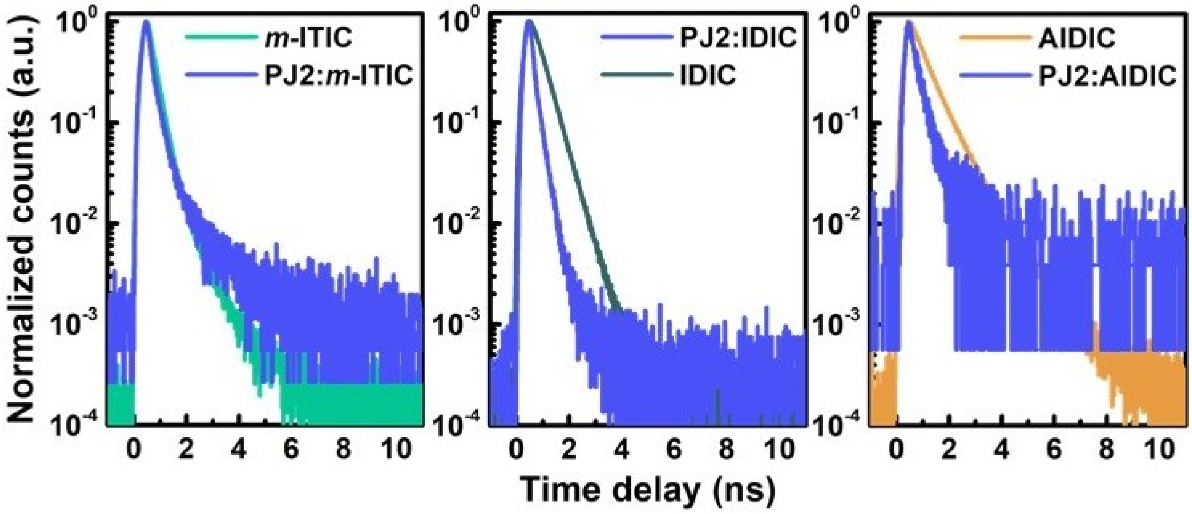

Fig. S17 The time-correlated single-photon counting (TCSPC) of neat acceptors and corresponding blend films, excited at 375 nm.

Table S4 The summary of $P(E,T)$ values under different conditions.

Devices	P (E, T) [%]	
	At short-circuit condition	At maximum power output condition
PJ1:*m*-ITIC	78.2	57.3
PJ1:IDIC	85.9	64.2
PJ1:AIDIC	–	–
PJ2:*m*-ITIC	91.7	68.6
PJ2:IDIC	94.1	79.3
PJ2:AIDIC	79.5	55.6
PJ3:*m*-ITIC	82.7	68.4
PJ3:IDIC	83.2	57.7
PJ3:AIDIC	–	–

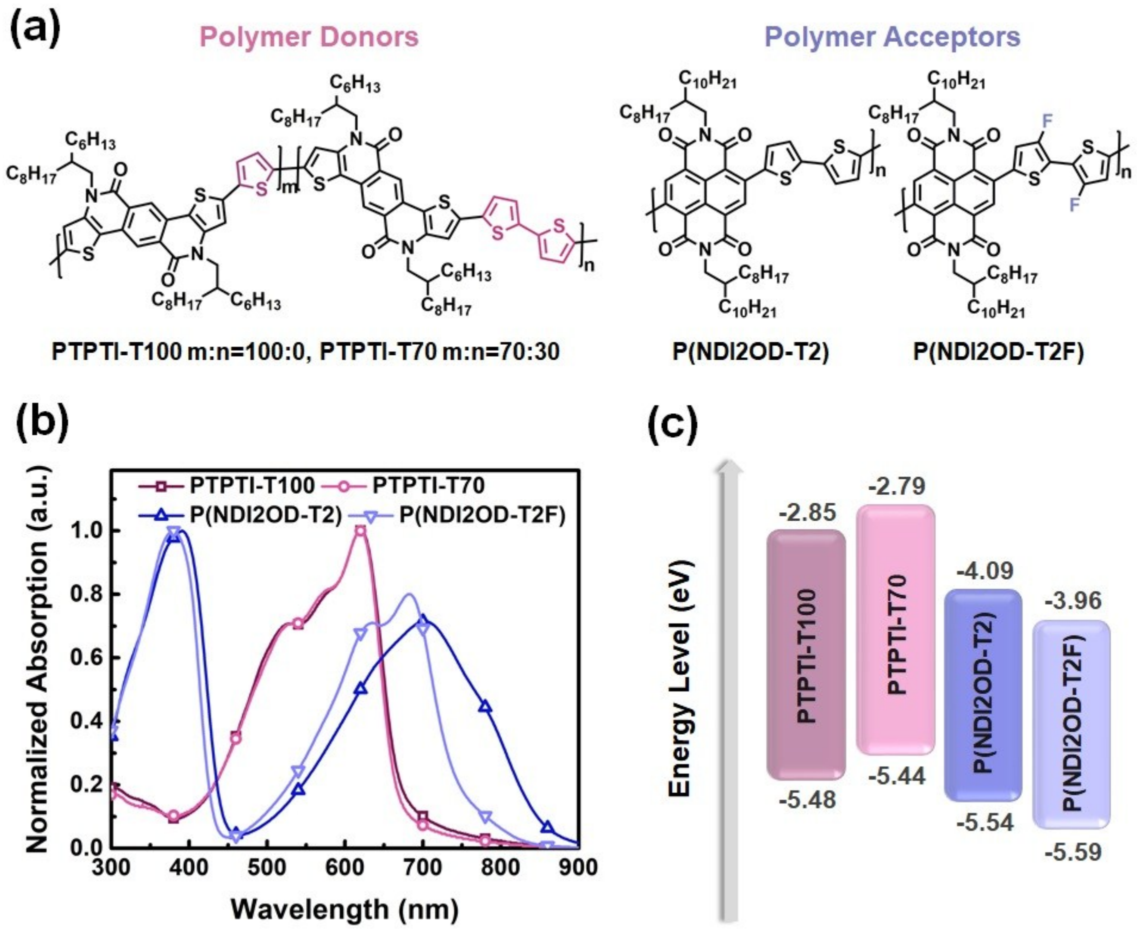

Fig. S18 (a) Chemical structures of polymer donors and acceptors used in this work. (b) Optical absorption spectra of neat films. (c) CV-derived energy level diagram.

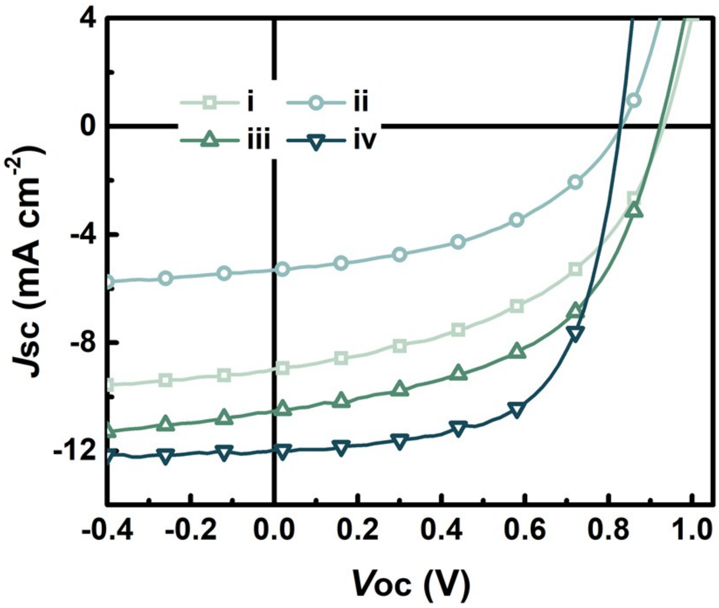

Fig. S19 The current density-voltage (*J-V*) curves for the all-PSCs based on PTPTI-Tx: acceptor (1.5:1, w/w): (i) PTPTI-T100:P(NDI2OD-T2), (ii) PTPTI-T100:P(NDI2OD-T2F), (iii) PTPTI-T70:P(NDI2OD-T2), and (iv) PTPTI-T70:P(NDI2OD-T2F) under the illumination of AM1.5G, 100 mW cm^{-2}.

Table S5. Photovoltaic parameters of the all-PSCs based on PTPTI-Tx: acceptor (1.5:1, w/w) under the illumination of AM1.5G, 100 mW cm^{-2}

Devices	Donor:Aaacptor	V_{oc} (V)[a]	J_{sc} (mA cm^{-2})[a]	FF (%)[a]	PCE (%)[a]
i	PTPTI-T100:P(NDI2OD-T2)	0.931 (0.925±0.007)	9.0 (8.9±0.2)	47.5 (46.9±0.6)	3.96 (3.83±0.17)
ii	PTPTI-T100:P(NDI2OD-T2F)	0.831 (0.830±0.003)	5.3 (5.3±0.1)	45.9 (45.2±0.8)	2.02 (1.88±0.14)
iii	PTPTI-T70:P(NDI2OD-T2)	0.923 (0.921±0.004)	10.5 (10.3±0.2)	52.0 (51.7±0.7)	5.05 (4.93±0.14)
iv	PTPTI-T70:P(NDI2OD-T2F)	0.828 (0.827±0.003)	12.0 (11.7±0.2)	62.5 (62.0±0.6)	6.19 (6.06±0.11)

[a]The average values are obtained from 15 devices with standard deviation.

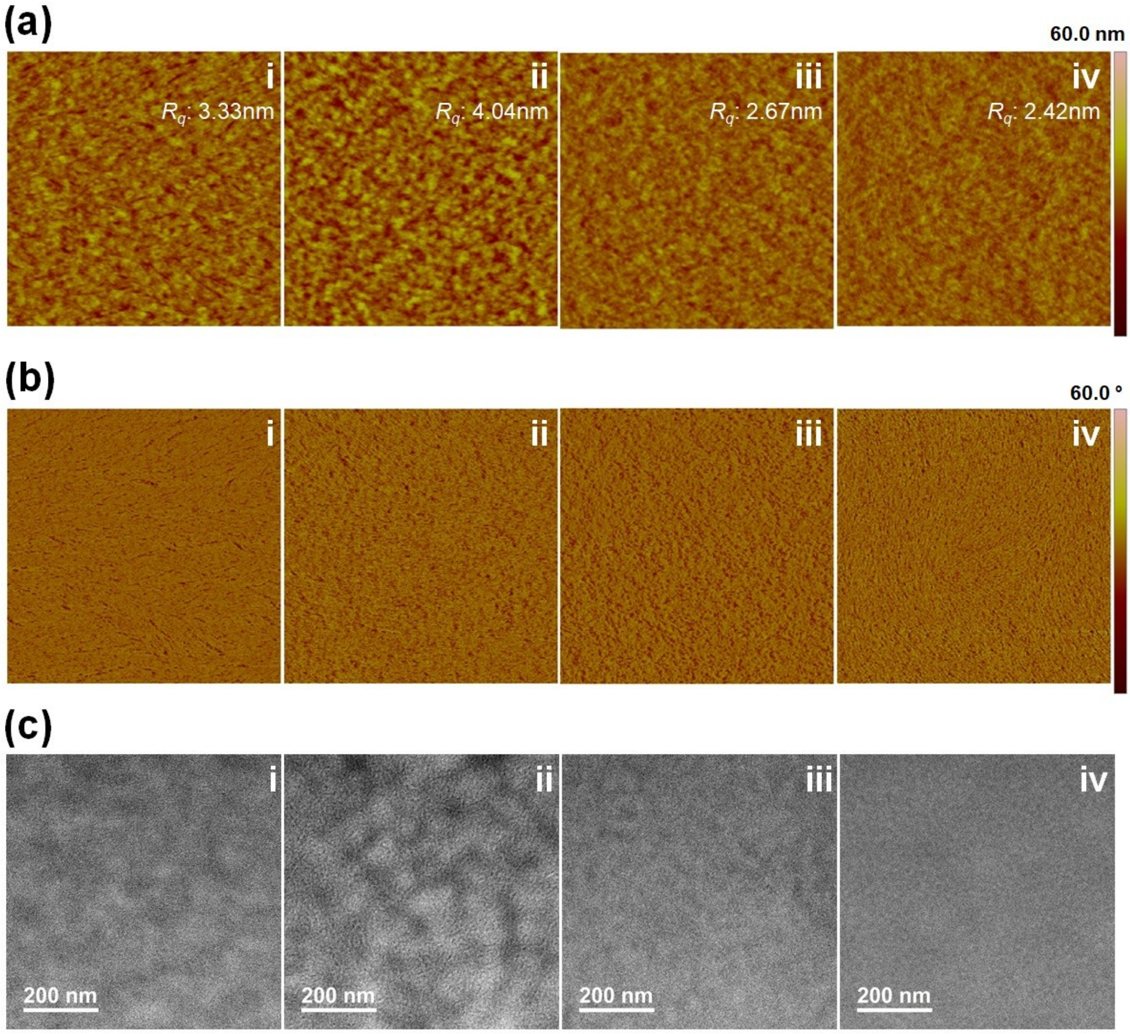

Fig. S20 (a) The AFM height images, (b) AFM phase images in 4μm × 4μm, and (c) TEM images of the blend films: (i) PTPTI-T100:P(NDI2OD-T2), (ii) PTPTI-T100:P(NDI2OD-T2F), (iii) PTPTI-T70:P(NDI2OD-T2), and (iv) PTPTI-T70:P(NDI2OD-T2F).

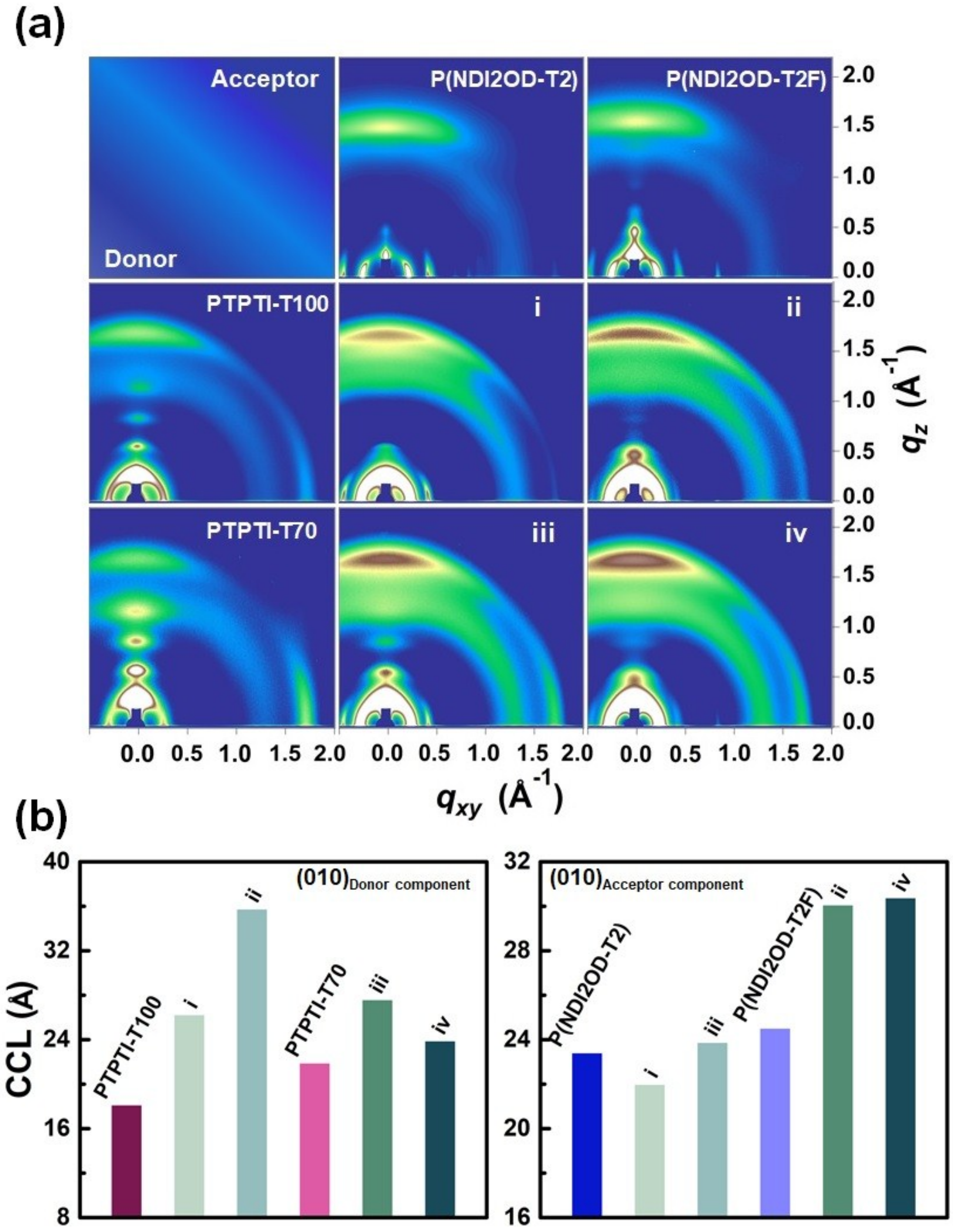

Fig. S21 (a) GIWAXS images of the neat and blend films: (i) PTPTI-T100:P(NDI2OD-T2), (ii) PTPTI-T100:P(NDI2OD-T2F), (iii) PTPTI-T70:P(NDI2OD-T2), and (iv) PTPTI-T70:P(NDI2OD-T2F); and (b) corresponding donor and acceptor components CCLs estimated from the face-on (010) diffractions.

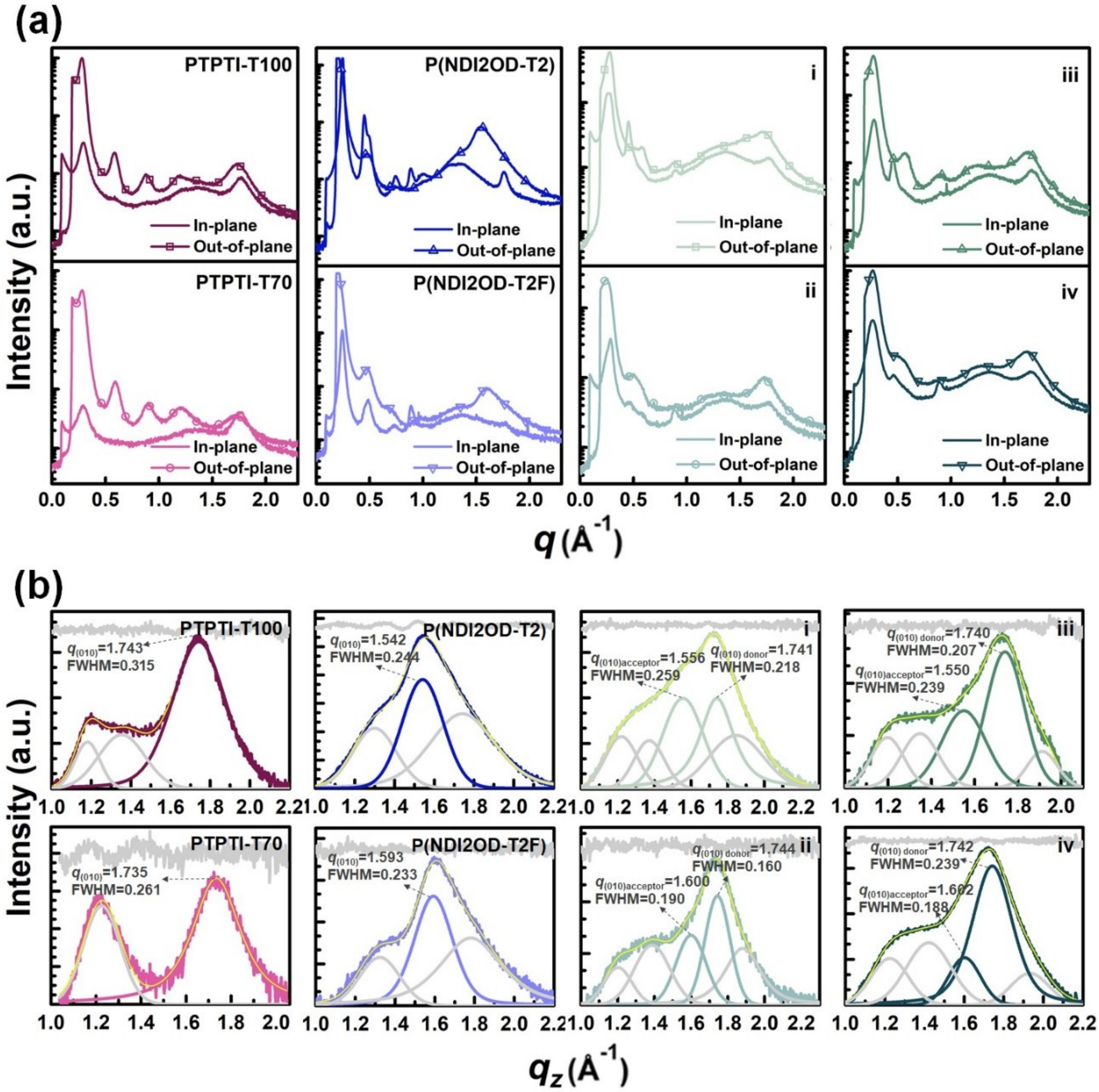

Fig. S22 (a) Line cuts of the GIWAXS images of the neat and blend films: (i) PTPTI-T100:P(NDI2OD-T2), (ii) PTPTI-T100:P(NDI2OD-T2F), (iii) PTPTI-T70:P(NDI2OD-T2), and (iv) PTPTI-T70:P(NDI2OD-T2F); and (b) corresponding multi-peak fits of the out-of-plane GIWAXS line cuts at the high region for the neat and blend films.

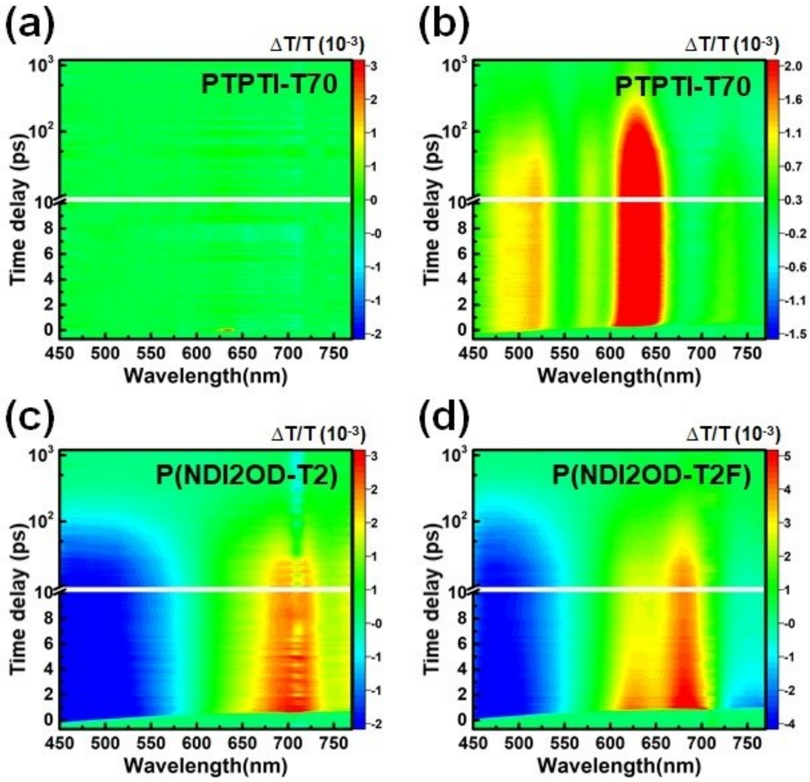

Fig. S23 TA dynamics recorded from (a) neat PTPTI-T70 with pump at 710 nm, (b) neat PTPTI-T70 with pump at 500 nm, (c) neat P(NDI2OD-T2) with pump at 710 nm, and (d) neat P(NDI2OD-T2F) with pump at 710 nm.

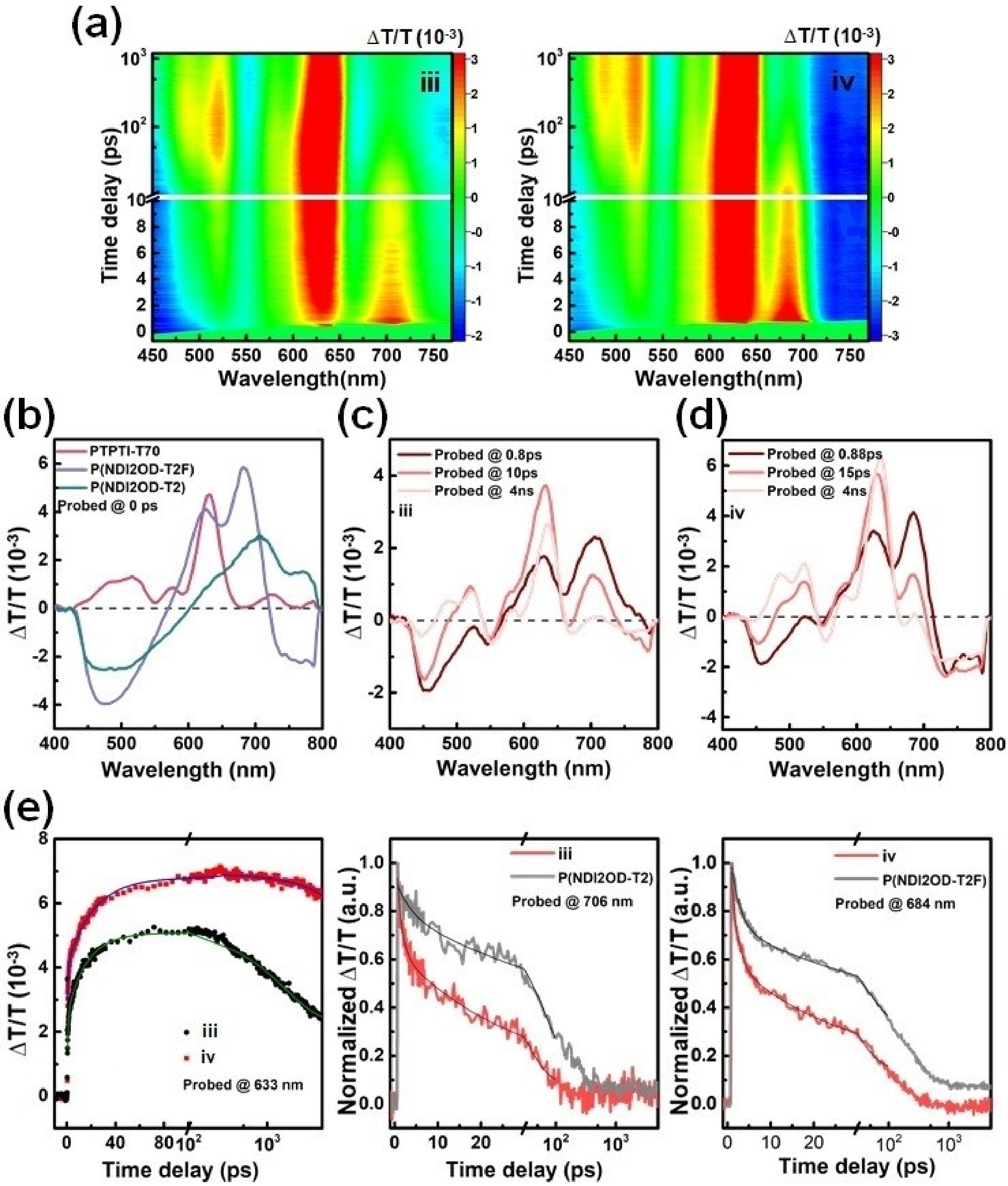

Fig. S24 (a) TA dynamics recorded from blend films with pump at 710 nm: (iii) PTPTI-T70:P(NDI2OD-T2), and (iv) PTPTI-T70:P(NDI2OD-T2F). (b) TA dynamics recorded from the neat film at 0 ps. (c) TA dynamics recorded from PTPTI-T70:P(NDI2OD-T2) blend film at different time delays. (d) TA dynamics recorded from PTPTI-T70:P(NDI2OD-T2F) blend film at different time delays. (e) The kinetic curves of the neat acceptor and corresponding blend films probed at different wavelength.

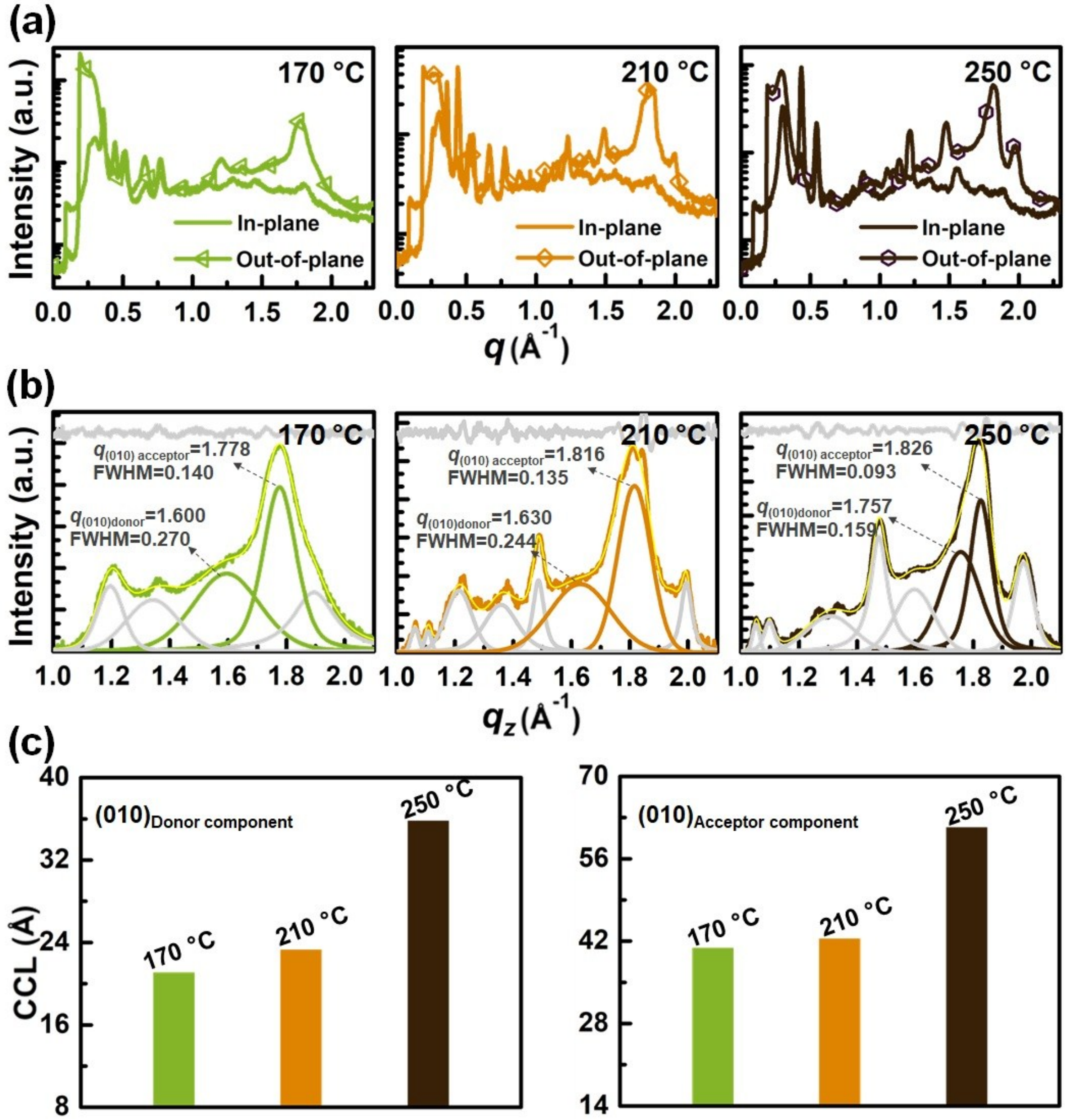

Fig. S25 (a) Line cuts of the GIWAXS images, (b) multi-peak fits at the high region along the out-of-plane direction, and (c) corresponding donor and acceptor components CCLs of the PJ2:IDIC blend films exposed at different temperatures (170, 210, and 250 °C).

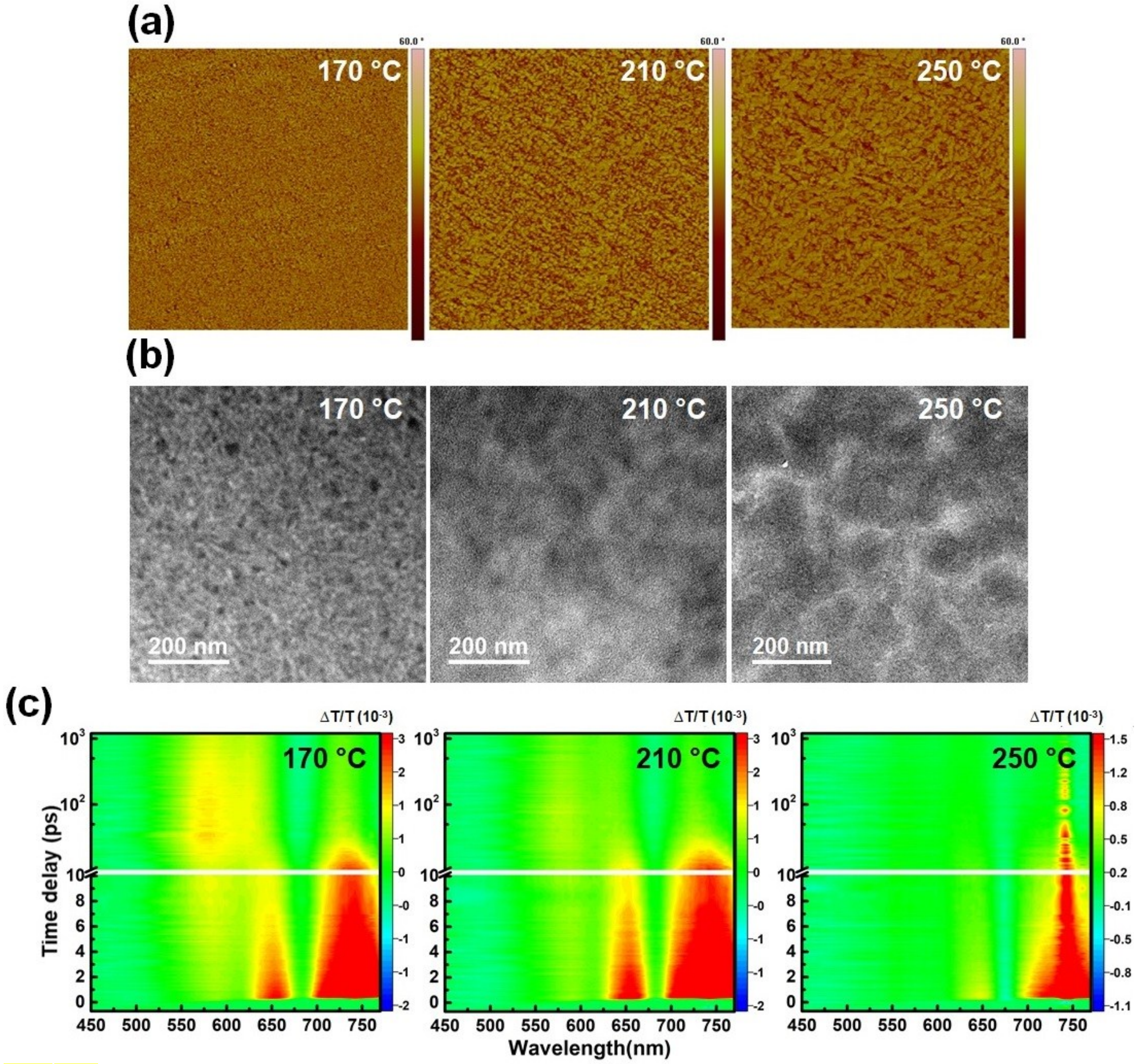

Fig. S26 (a) AFM phase images, (b) TEM images, and (c) transient absorption (TA) dynamics recorded with pump at 740 nm of the PJ2:IDIC blend films exposed at different temperatures (170, 210, and 250 °C).

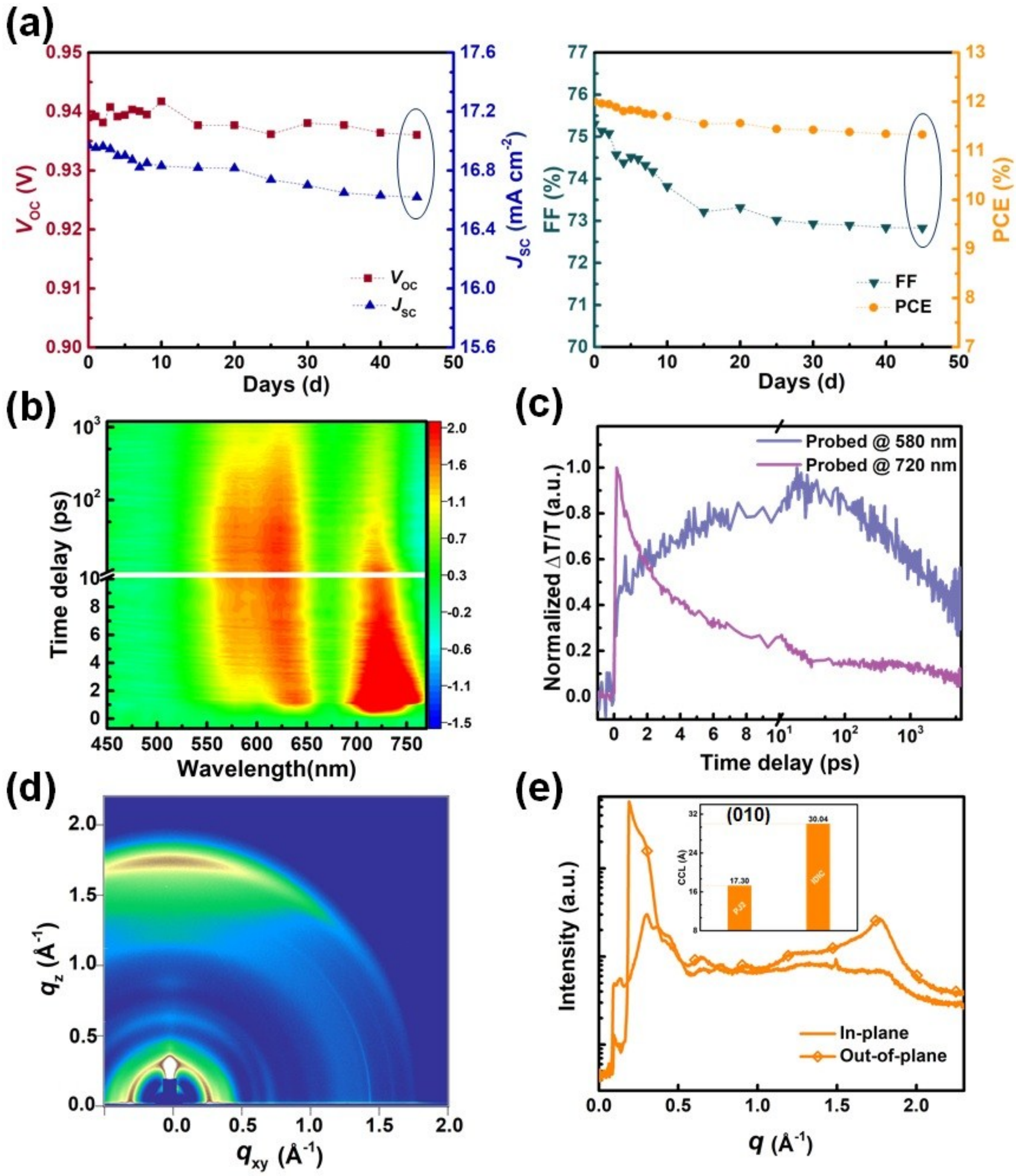

Fig. S27 (a) Long-term stability of the PJ2:IDIC based NF-PSCs in inert condition without encapsulation. (b) Transient absorption (TA) dynamics recorded with pump at 740 nm from the PJ2:IDIC blend film after 45 days storage in inert condition without encapsulation and (c) the corresponding normalized dynamic curve probed at 580 nm and 720 nm. (d) The GIWAXS image of the PJ2:IDIC blend film after 45 days storage in the same condition and (e) the corresponding line cuts, insert: CCLs (17.30 Å for PJ2, 30.04 Å for IDIC) estimated from the face-on (010) diffractions.

Table S6 Photovoltaic parameters of the NF-PSCs based on PJ1:SMAs with different D/A weight ratios in CF.

active layer	D/A ration	V_{OC} [V]	J_{SC} [mA cm^{-2}]	FF [%]	PCE [%]
PJ1:*m*-ITIC	1:1	1.031	8.5	48.3	4.23
	1:1.5	1.040	9.3	50.0	4.81
	1:2	1.039	9.3	47.5	4.59
PJ1:IDIC	1:1	0.964	9.0	40.0	3.46
	1:1.5	0.965	9.9	48.1	4.57
	1:2	0.962	9.9	45.7	4.36
PJ1:AIDIC	1:1	0.968	3.2	34.2	1.05
	1:1.5	0.964	4.0	37.9	1.46
	1:2	0.964	3.9	35.2	1.33

Table S7 Photovoltaic parameters of the NF-PSCs based on PJ2:SMAs with different D/A weight ratios in CF.

active layer	D/A ration	V_{OC} [V]	J_{SC} [mA cm^{-2}]	FF [%]	PCE [%]
PJ2:*m*-ITIC	1:1	0.992	12.8	49.9	6.31
	1:1.5	0.995	13.7	51.7	7.03
	1:2	0.994	13.7	50.3	6.85
PJ2:IDIC	1:1	0.940	15.1	59.8	8.47
	1:1.5	0.942	15.8	59.5	8.86
	1:2	0.941	15.8	56.8	8.43
PJ2:AIDIC	1:1	0.963	9.0	40.0	3.45
	1:1.5	0.965	9.4	42.6	3.88
	1:2	0.962	9.2	40.1	3.56

Table S8 Photovoltaic parameters of the NF-PSCs based on PJ3:SMAs with different D/A weight ratios in CF.

active layer	D/A ration	V_{OC} [V]	J_{SC} [mA cm^{-2}]	FF [%]	PCE [%]
PJ3:*m*-ITIC	1:1	0.967	10.2	44.2	4.37
	1:1.5	0.964	11.0	48.7	5.18
	1:2	0.963	11.1	45.4	4.86
PJ3:IDIC	1:1	0.915	10.9	50.1	4.98
	1:1.5	0.915	11.2	54.3	5.54
	1:2	0.914	11.1	52.2	5.28
PJ3:AIDIC	1:1	0.870	3.7	38.1	1.22
	1:1.5	0.872	4.0	40.3	1.40
	1:2	0.872	3.9	38.3	1.31

Table S9 Photovoltaic parameters of the NF-PSCs based on PJ1:SMAs (D/A=1/1.5) different amounts of DIO additive in CF.

active layer	additive	V_{OC} [V]	J_{SC} [mA cm^{-2}]	FF [%]	PCE [%]
PJ1:*m*-ITIC	0.25%	1.043	10.5	50.4	5.51
	0.5%	1.041	10.9	53.0	6.01
	1%	1.041	10.9	50.1	5.65
PJ1:IDIC	0.25%	0.961	10.9	49.0	5.15
	0.5%	0.960	11.1	50.1	5.35
	1%	0.961	10.9	50.0	5.22
PJ1:AIDIC	0.25%	0.963	4.3	40.0	1.65
	0.5%	0.962	4.9	40.1	1.90
	1%	0.964	4.8	40.2	1.88

Table S10 Photovoltaic parameters of the NF-PSCs based on PJ2:SMAs (D/A=1/1.5) different amounts of DIO additive in CF.

active layer	additive	V_{OC} [V]	J_{SC} [mA cm^{-2}]	FF [%]	PCE [%]
PJ2:*m*-ITIC	0.25%	0.993	14.9	55.2	8.13
	0.5%	0.994	15.6	59.4	9.23
	1%	0.991	15.5	57.7	8.85
PJ2:IDIC	0.25%	0.940	16.0	62.5	9.41
	0.5%	0.939	16.6	66.0	10.25
	1%	0.937	16.6	65.0	10.09
PJ2:AIDIC	0.25%	0.962	10.1	47.1	4.58
	0.5%	0.960	10.9	50.0	5.23
	1%	0.961	10.9	49.8	5.21

Table S11 Photovoltaic parameters of the NF-PSCs based on PJ3:SMAs (D/A=1/1.5) different amounts of DIO additive in CF.

active layer	additive	V_{OC} [V]	J_{SC} [mA cm^{-2}]	FF [%]	PCE [%]
PJ3:*m*-ITIC	0.25%	0.964	11.8	50.8	5.76
	0.5%	0.967	11.7	56.0	6.32
	1%	0.965	11.6	55.1	6.14
PJ3:IDIC	0.25%	0.911	11.8	59.0	6.35
	0.5%	0.913	11.9	61.1	6.63
	1%	0.913	11.3	60.0	6.17
PJ3:AIDIC	0.25%	0.869	4.1	42.1	1.48
	0.5%	0.872	4.3	44.9	1.69
	1%	0.868	4.1	38.0	1.35

Table S12 Photovoltaic parameters of the NF-PSCs based on PJ1:SMAs (D/A=1/1.5 CF/DIO=1/0.5%) with different annealing temperatures.

active layer	T [^{o}C]	V_{OC} [V]	J_{SC} [mA cm^{-2}]	FF [%]	PCE [%]
PJ1:*m*-ITIC	110	1.040	11.0	55.4	6.36
	130	1.031	11.1	56.0	6.41
	150	1.027	10.4	50.1	5.34
PJ1:IDIC	110	0.959	11.9	54.0	6.16
	130	0.958	12.0	53.6	6.18
	150	0.953	11.3	52.1	5.59
PJ1:AIDIC	110	0.960	5.3	40.1	2.04
	130	0.961	5.3	40.6	2.06
	150	0.960	5.1	40.1	1.97

Table S13 Photovoltaic parameters of the NF-PSCs based on PJ2:SMAs (D/A=1/1.5 CF/DIO=1/0.5%) with different annealing temperatures.

active layer	T [^{o}C]	V_{OC} [V]	J_{SC} [mA cm^{-2}]	FF [%]	PCE [%]
PJ2:*m*-ITIC	110	0.990	16.5	60.2	9.80
	130	0.988	16.8	62.3	10.34
	150	0.982	16.6	61.6	10.01
PJ2:IDIC	110	0.937	16.7	72.1	11.31
	130	0.939	17.0	75.3	12.01
	150	0.937	16.3	74.9	11.46
PJ2:AIDIC	110	0.957	11.2	50.2	5.37
	130	0.958	11.4	50.9	5.56
	150	0.950	11.1	50.3	5.28

Table S14 Photovoltaic parameters of the NF-PSCs based on PJ3:SMAs (D/A=1/1.5 CF/DIO=1/0.5%) with different annealing temperatures.

active layer	T [^{o}C]	V_{OC} [V]	J_{SC} [mA cm^{-2}]	FF [%]	PCE [%]
PJ3:*m*-ITIC	110	0.964	12.1	59.8	6.97
	130	0.960	12.7	63.5	7.76
	150	0.960	12.5	60.7	7.25
PJ3:IDIC	110	0.909	12.3	67.0	7.50
	130	0.908	12.8	69.8	8.11
	150	0.901	12.7	68.3	7.82
PJ3:AIDIC	110	0.870	4.4	50.1	1.89
	130	0.867	4.7	55.4	2.25
	150	0.858	4.5	52.5	2.03

References

[1] Comyn, J. Int. J. *Adhes. Adhes.* 1992, **12**, 145-149.

[2] S. Wu, J. Polym. Sci., Part C: *Polym. Symp.* 1971, **34**, 19.